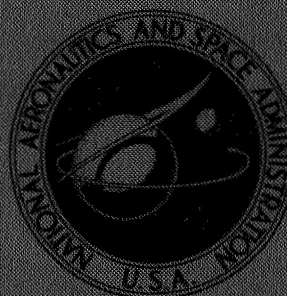


# NASA TECHNICAL MEMORANDUM



NASA TM X-1621

NASA TM X-1621

FACILITY FORM 602

**N 68-30030**

(ACCESSION NUMBER)

(THRU)

**35**

(PAGES)

**1**

(CODE)

**01**

(CATEGORY)

(NASA CR OR TMX OR AD NUMBER)

GPO PRICE \$ \_\_\_\_\_

CFSTI PRICE(S) \$ \_\_\_\_\_

Hard copy (HC) **\$ 3.00**

Microfiche (MF) **\$ .65**

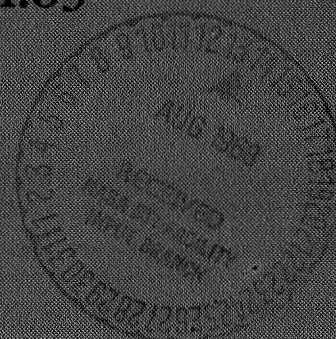
ff 653 July 65

## AERODYNAMIC CHARACTERISTICS OF TWO BLUNT, HALF-CONE—WEDGE ENTRY CONFIGURATIONS AT MACH NUMBERS FROM 2.30 TO 4.63

*by Gerald V. Foster*

*Langley Research Center*

*Langley Station, Hampton, Va.*





AERODYNAMIC CHARACTERISTICS OF TWO BLUNT,  
HALF-CONE—WEDGE ENTRY CONFIGURATIONS  
AT MACH NUMBERS FROM 2.30 TO 4.63

By Gerald V. Foster

Langley Research Center  
Langley Station, Hampton, Va.

NATIONAL AERONAUTICS AND SPACE ADMINISTRATION

---

For sale by the Clearinghouse for Federal Scientific and Technical Information  
Springfield, Virginia 22151 - CFSTI price \$3.00

AERODYNAMIC CHARACTERISTICS OF TWO BLUNT,  
HALF-CONE—WEDGE ENTRY CONFIGURATIONS  
AT MACH NUMBERS FROM 2.30 TO 4.63

By Gerald V. Foster  
Langley Research Center

SUMMARY

An investigation has been conducted in the Langley Unitary Plan wind tunnel to determine the aerodynamic characteristics in combined pitch and sideslip for two blunt, half-cone—wedge entry vehicles at Mach numbers from 2.30 to 4.63. The vehicles differed primarily in length.

The results of the investigation indicated that both configurations were longitudinally stable although the drag level was greater for the short configuration. Both configurations exhibited positive directional stability and a positive dihedral effect throughout the ranges of angle of attack and Mach number; however, the parameters for the long configuration varied considerably with angle of attack.

INTRODUCTION

The Langley Research Center is expending considerable effort on the varied problems associated with lifting entry vehicles. For the purpose of economy and expediency, interest has been directed toward a lifting entry vehicle which would serve as a test bed for evaluations of new concepts, materials, and subsystems. The test vehicle is to be rocket launched and guided along a preselected entry trajectory. One proposed configuration for a test vehicle consists of a half-cone—wedge-body combination with a hemispherical nose and a guidance system utilizing lateral center-of-gravity movement. As part of an investigation of this concept, it was desirable to determine the basic aerodynamic characteristics of the vehicle in order to ascertain the effects of lateral center-of-gravity movement on the guidance capability.

Accordingly, an investigation has been undertaken at the Langley Unitary Plan wind tunnel to determine the aerodynamic characteristics of two blunt, half-cone—wedge entry models through a Mach number range from 2.30 to 4.63. The models, although different in length, had identical base dimensions. Tests were made through a range of angle of attack from about  $-50^{\circ}$  to  $50^{\circ}$  at angles of sideslip from about  $-4^{\circ}$  to  $6^{\circ}$ , and through a

range of angle of sideslip from about  $-5^\circ$  to  $50^\circ$  at angles of attack of about  $-9^\circ$ ,  $0^\circ$ , and  $10^\circ$ . The Reynolds number per foot was  $1.0 \times 10^6$  (per meter,  $3.28 \times 10^6$ ).

## SYMBOLS

The results are presented as force and moment coefficients. All coefficients are referred to the body-axis system with the moment reference located at 61.2 percent body length for the short model and at 44.8 percent body length for the long model.

$b$  body reference span, 6.6 inches (16.76 centimeters)

$C_A$  axial-force coefficient,  $\frac{\text{Axial force}}{qS}$

$C_l$  rolling-moment coefficient,  $\frac{\text{Rolling moment}}{qSb}$

$C_{l\beta}$  rolling-moment parameter,  $\frac{\Delta C_l}{\Delta \beta}$ , per degree

$C_m$  pitching-moment coefficient,  $\frac{\text{Pitching moment}}{qSb}$

$C_{m\alpha}$  slope of pitching-moment curve per degree

$C_N$  normal-force coefficient,  $\frac{\text{Normal force}}{qS}$

$C_{N\alpha}$  slope of normal-force curve per degree

$C_n$  yawing-moment coefficient,  $\frac{\text{Yawing moment}}{qSb}$

$C_{n\beta}$  yawing-moment parameter,  $\frac{\Delta C_n}{\Delta \beta}$ , per degree

$C_{p,b}$  base pressure coefficient,  $\frac{\text{Base pressure}}{qS}$

$C_Y$  side-force coefficient,  $\frac{\text{Side force}}{qS}$

$C_{Y\beta}$  side-force parameter,  $\frac{\Delta C_Y}{\Delta \beta}$ , per degree



$l$	body length
$M$	Mach number
$q$	free-stream dynamic pressure
$S$	reference area taken at base of model, 0.228 foot <sup>2</sup> (0.0212 meter <sup>2</sup> )
$x$	coordinate measured from body leading edge
$\alpha$	angle of attack referred to body reference line, degrees
$\beta$	angle of sideslip referred to plane of symmetry of body, degrees

### MODELS AND APPARATUS

Details of the models are presented in figure 1 and photographs are presented in figure 2. Both models had flat tops and identical bases consisting of a combination of rectangular and semicircular sections. Since the models differed primarily in length, they are designated as the long and the short configurations.

The tests were made in the high Mach number test section of the Langley Unitary Plan wind tunnel which is a variable-pressure, continuous-flow tunnel. The models were mounted in the tunnel on a remotely controlled sting. Forces and moments were measured by means of a six-component internal strain-gage balance.

### TESTS AND CORRECTIONS

The conditions for the tests were as follows:

M	Stagnation pressure		Stagnation temperature		Reynolds number	
	psia	kN/m <sup>2</sup>	°F	°K	per foot	per meter
2.30	5.3	36.54	150	338	$1.0 \times 10^6$	$3.28 \times 10^6$
2.96	7.5	51.71	150	338	1.0	3.28
3.95	13.3	91.70	175	352	1.0	3.28
4.63	18.3	126.17	175	352	1.0	3.28

The stagnation dewpoint was maintained sufficiently low (-30° F (239° K) or less) to assure negligible condensation effects in the test section.

Tests were obtained through a range of angle of attack from about  $-50^\circ$  to  $50^\circ$  at angles of sideslip from about  $-4^\circ$  to  $6^\circ$  and through a range of sideslip angle from about  $-5^\circ$  to  $50^\circ$  at angles of attack of about  $-9^\circ$ ,  $0^\circ$ , and  $10^\circ$ . The angles of attack and sideslip have been corrected for the deflection of the balance and sting under aerodynamic load and also for tunnel flow misalignment where applicable.

The base pressures were essentially the same for the two models at a given Mach number and were invariant with angle of attack. Variation of base pressure coefficient with Mach number was as follows:

Mach number	$C_{p,b}$
2.30	0.215
2.96	.153
3.95	.095
4.63	.081

The axial-force data presented in this paper do not include an adjustment for base pressure.

## PRESENTATION OF RESULTS

An outline of the contents of the data figures is as follows:

	Figure
Aerodynamic characteristics in pitch of long and short models:	
$\beta = 0^\circ$ . . . . .	3
Variation of longitudinal parameters with Mach number . . . . .	4
Variation of center-of-pressure position with $\alpha$ . . . . .	5
Aerodynamic characteristics in sideslip of long model . . . . .	6 to 9
Aerodynamic characteristics in sideslip of short model . . . . .	10 to 13
Variation of lateral-directional stability parameters with $\alpha$ . . . . .	14

## RESULTS AND DISCUSSION

The longitudinal aerodynamic characteristics for the long and short configurations are presented in figure 3 and summarized in figure 4. Both configurations are longitudinally stable. There is a general decrease in the slope of the normal force curve at the higher angles of attack that tends to decrease the stability level. (See fig. 3.) The results shown in figure 4 indicate that the longitudinal parameters for the long and short models have similar variations with Mach number. It may also be noted in this figure that the



axial force of the short model is at least 50 percent greater than that of the long model at all test Mach numbers. There appears to be little effect of Mach number on center-of-pressure locations for either the long or short model except for a range of angles of attack near  $C_N = 0$ . (See fig. 5.) For the high positive and negative angles of attack, the center of pressure of the long model is near the 65 percent body station, whereas the center of pressure of the short model is near the 75 percent body station.

The aerodynamic characteristics in sideslip at various angles of attack are shown in figures 6 to 9 for the long model and in figures 10 to 13 for the short model. There appear to be no large variations in the normal-force or pitching-moment characteristics in sideslip. The variations of yawing-moment, rolling-moment, and side-force coefficients with sideslip angle are reasonably linear for both models.

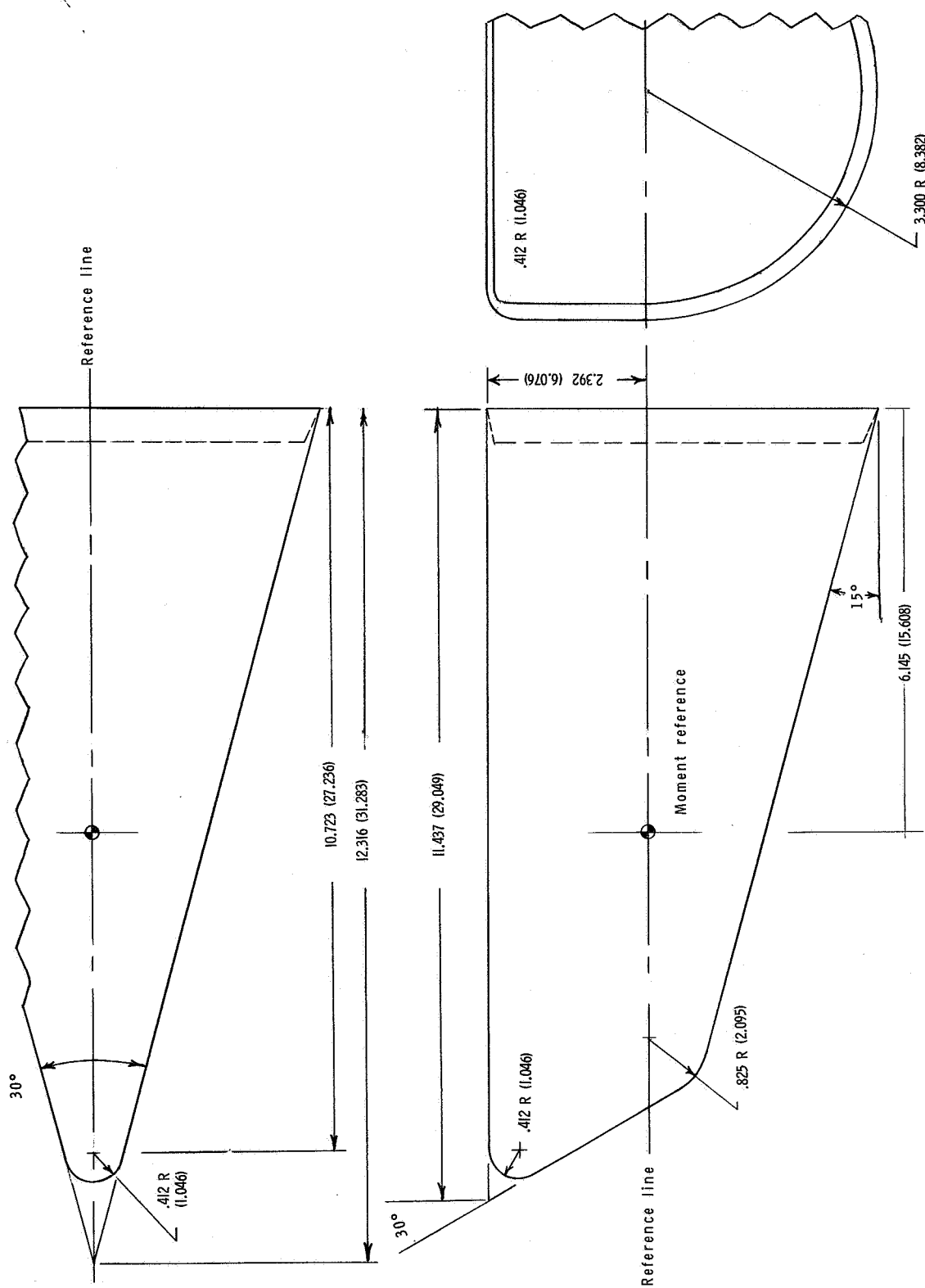
The variations of the lateral- and directional-stability parameters with angle of attack for both models are shown in figure 14. Although there is considerable variation of these parameters with angle of attack, the results, in general, indicate positive directional stability and a positive dihedral effect ( $-C_{l_\beta}$ ) throughout the ranges of angle of attack and Mach number for both models. In general, the effects of Mach number and angle of attack on the lateral-directional stability characteristics are less pronounced for the short model than for the long model.

#### CONCLUDING REMARKS

An investigation has been conducted in the Langley Unitary Plan wind tunnel to determine the aerodynamic characteristics in combined pitch and sideslip for two blunt, half-cone—wedge entry vehicles at Mach numbers from 2.30 to 4.63. The vehicles differed primarily in length.

The results of the investigation indicated that both models were longitudinally stable although the drag level was greater for the short model. Both models exhibited positive directional stability and a positive dihedral effect throughout the ranges of angle of attack and Mach number; however, the parameters for the long model varied considerably with angle of attack.

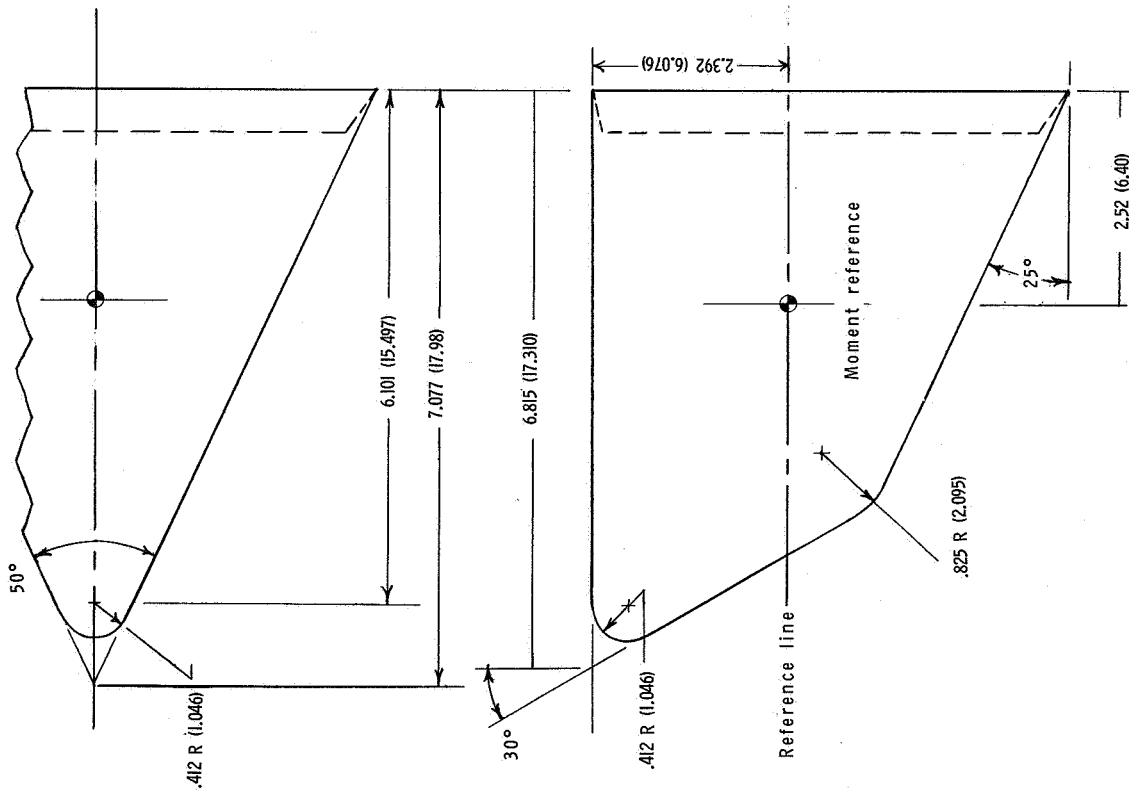
Langley Research Center,  
National Aeronautics and Space Administration,  
Langley Station, Hampton, Va., May 1, 1968,  
124-08-03-18-23.



(a) Long model.

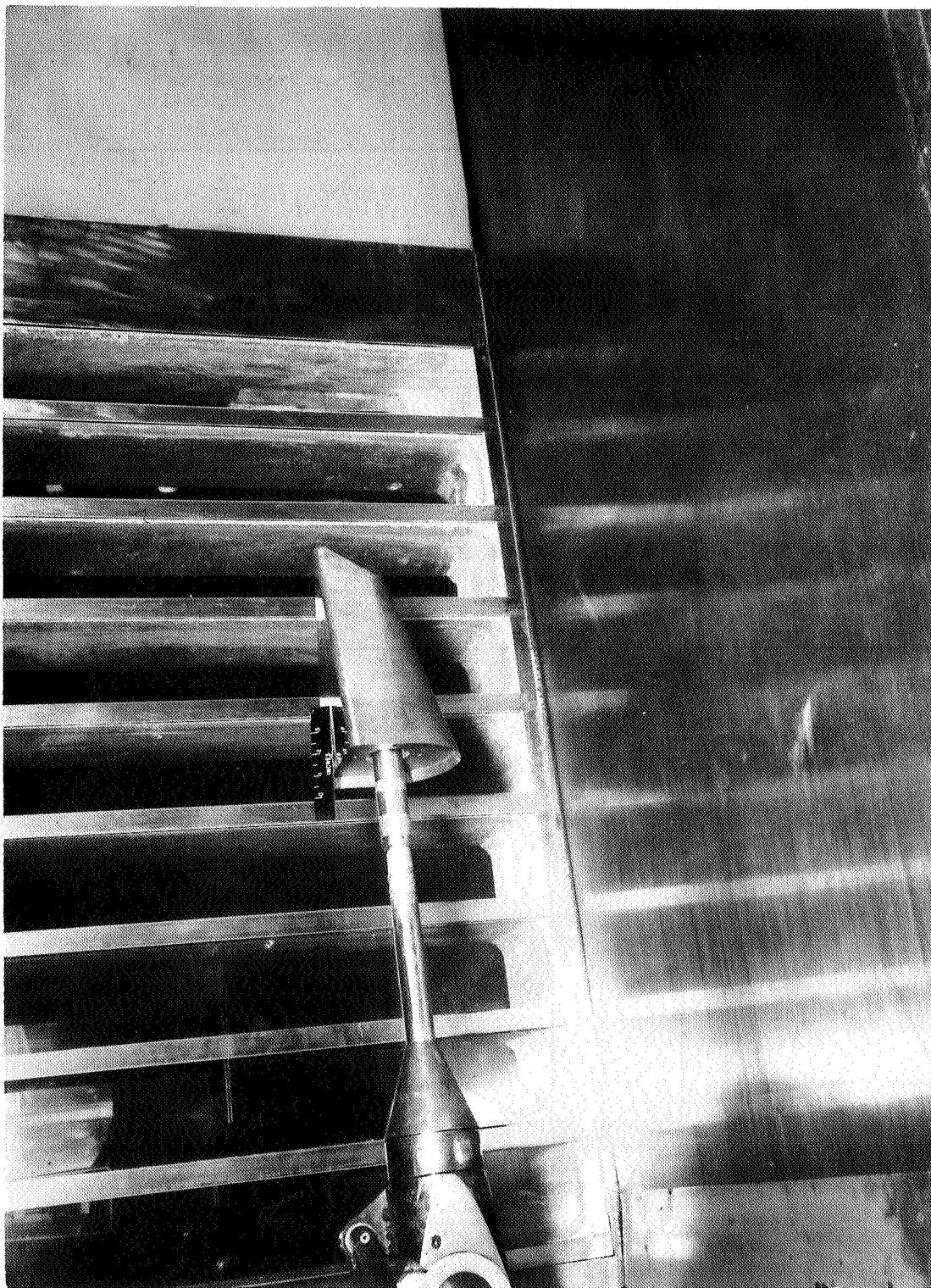
Figure 1.- Details of models. All dimensions are given, in inches and parenthetically in centimeters unless otherwise noted.





(b) Short model.

Figure 1.- Concluded.

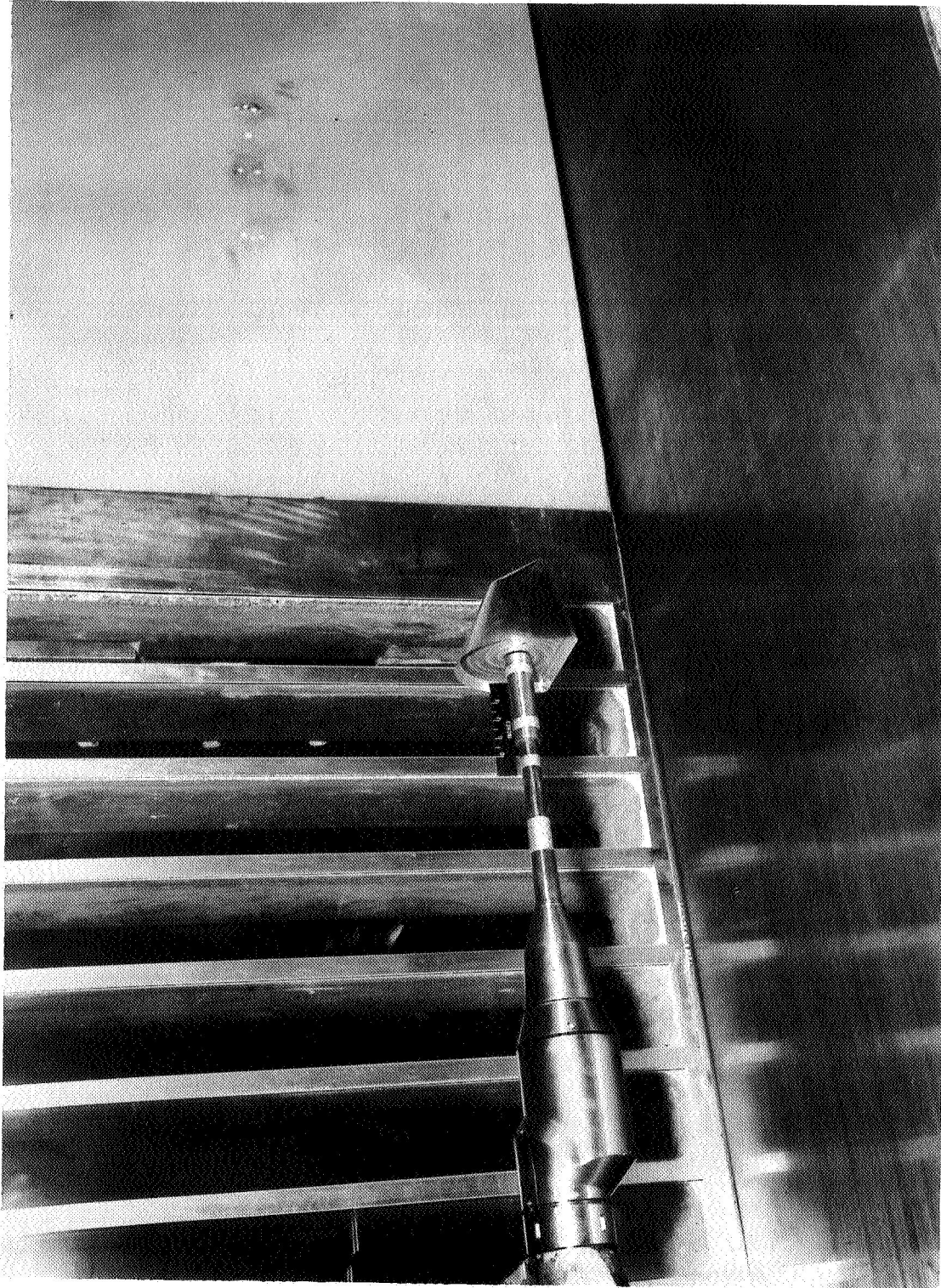


(a) Long model.

Figure 2.- Photographs of models mounted in wind tunnel.

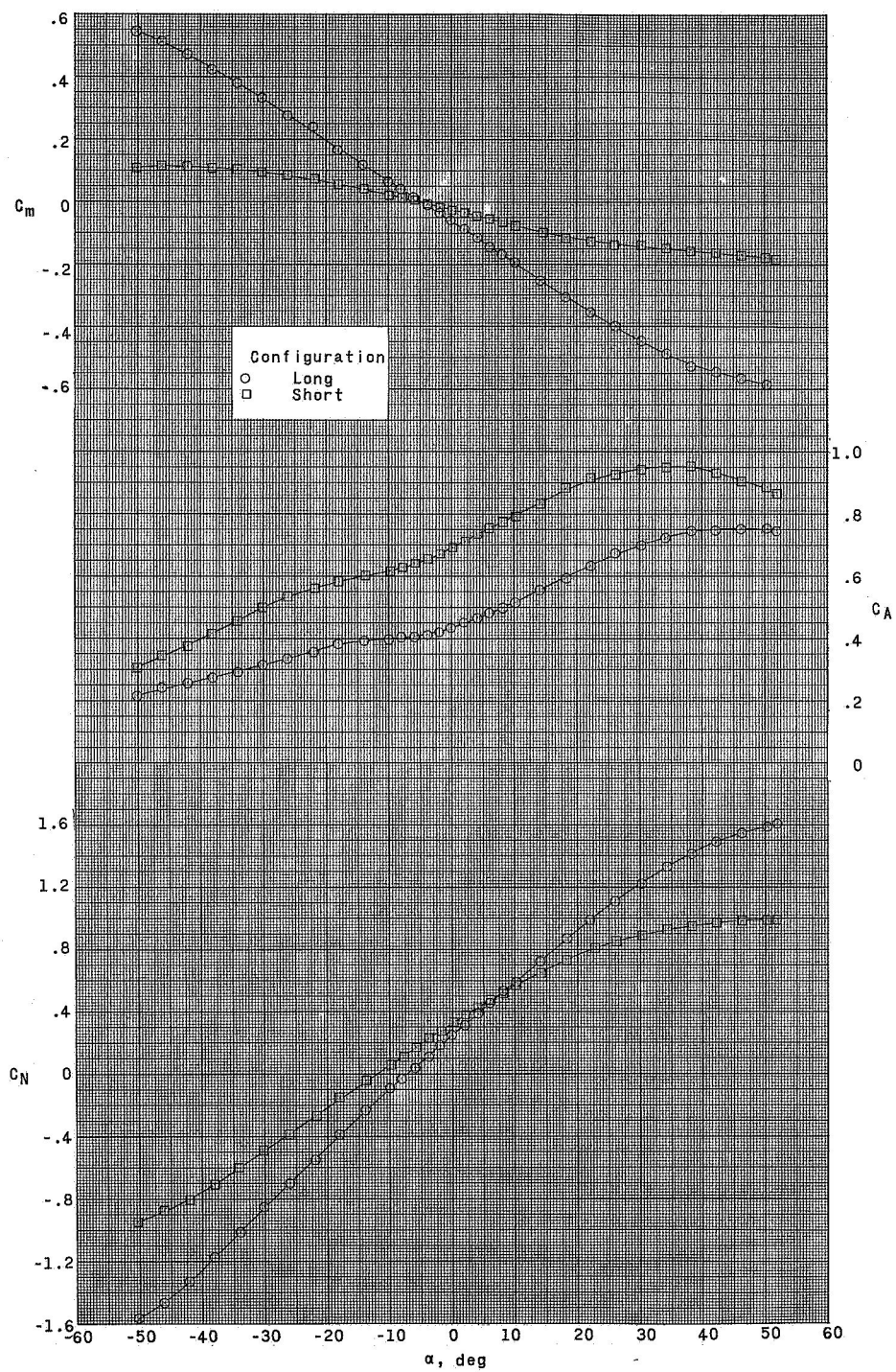
L-65-5573





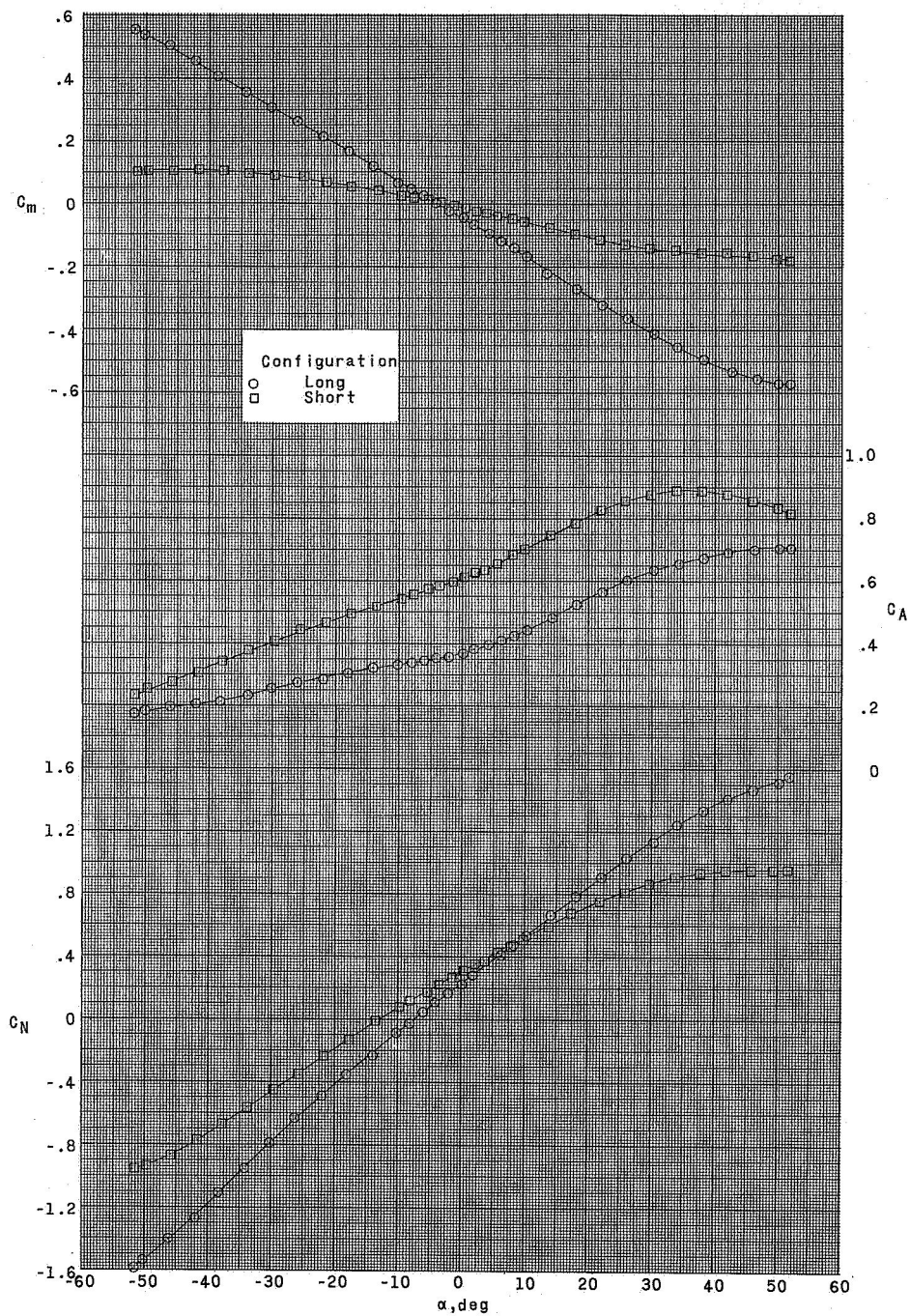
(b) Short model.  
Figure 2.- Concluded.

L-65-5269



(a)  $M = 2.30$ .

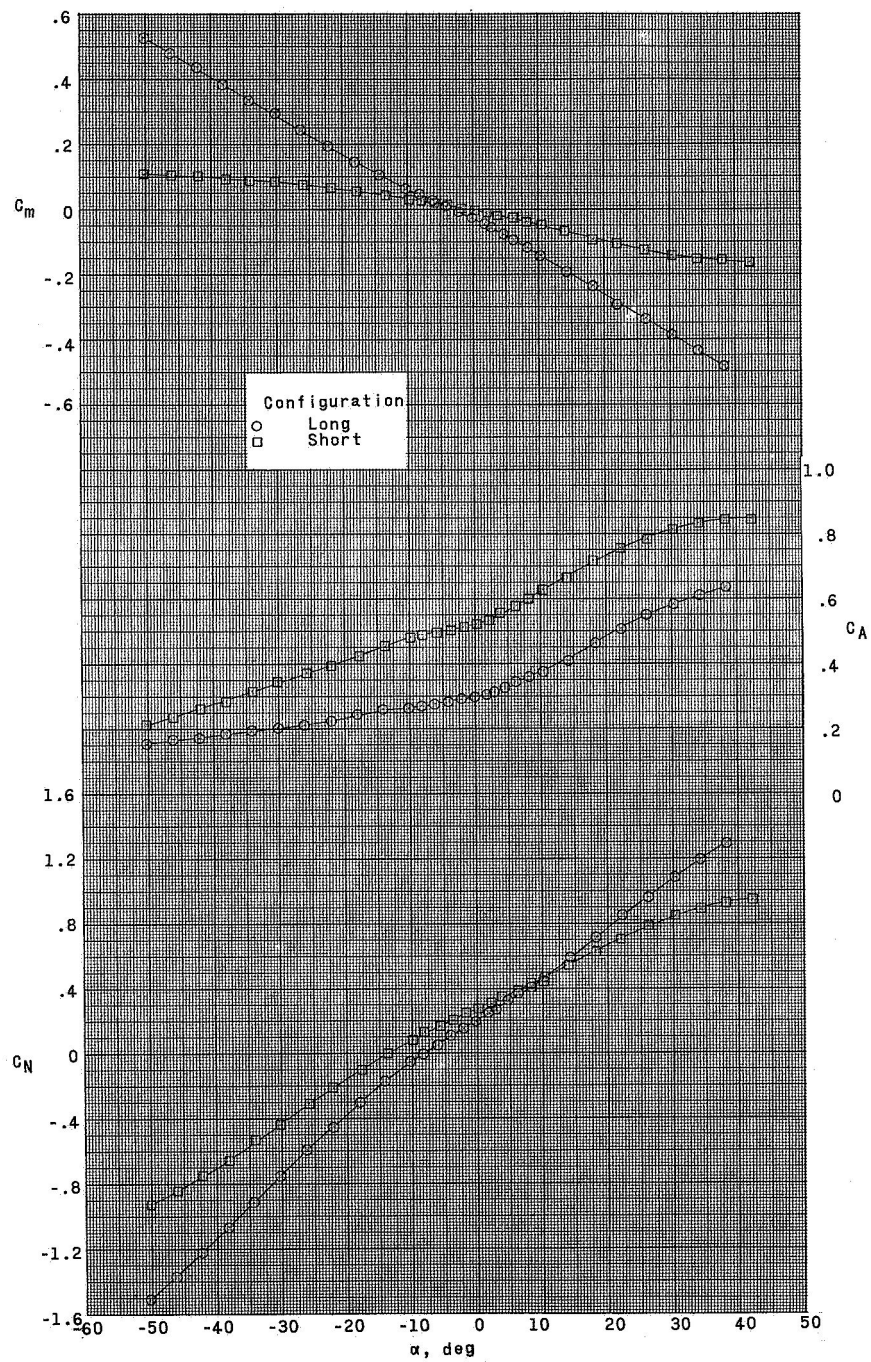
Figure 3.- Aerodynamic characteristics of long and short configurations in pitch.  $\beta = 0^\circ$ .



(b)  $M = 2.96$ .

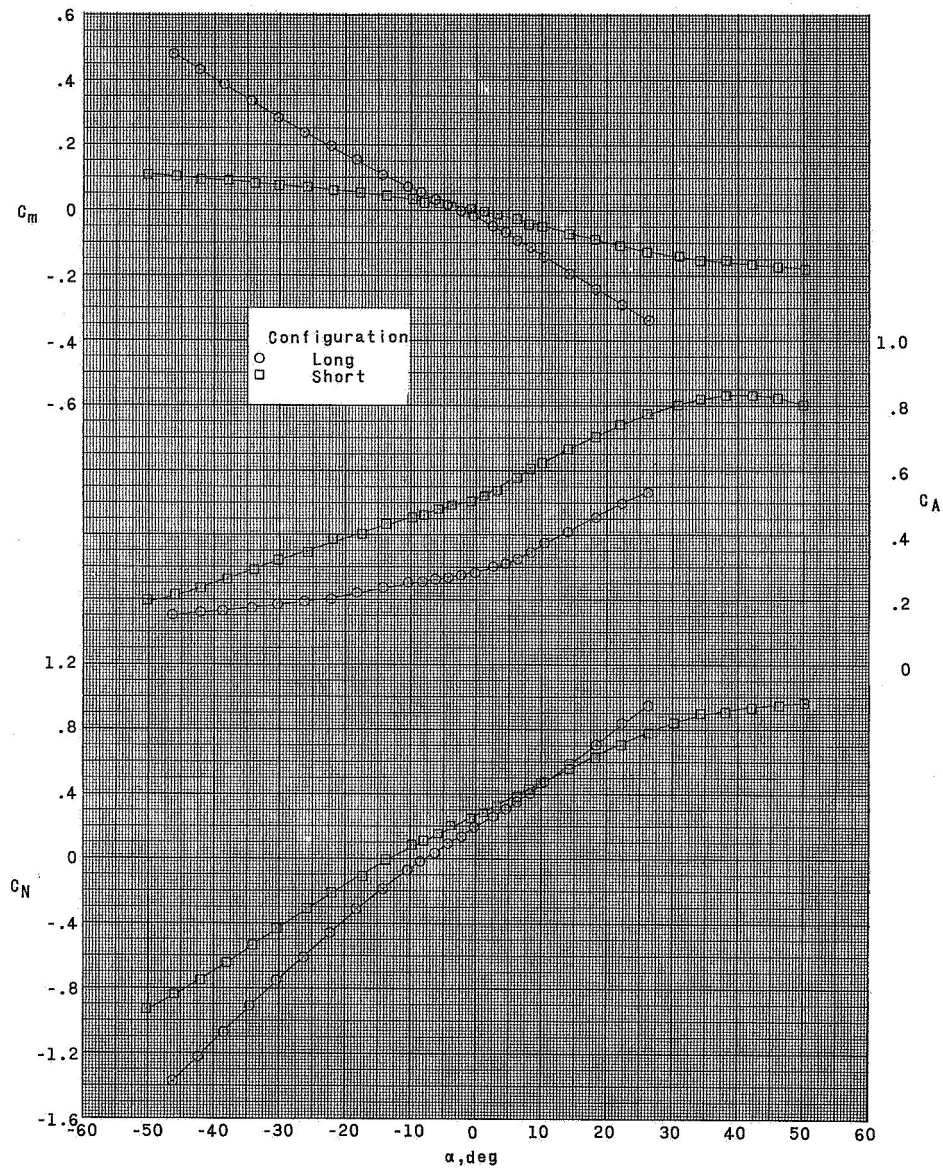
Figure 3.- Continued.





(c)  $M = 3.95$ .

Figure 3.- Continued.



(d)  $M = 4.63$ .

Figure 3.- Concluded.

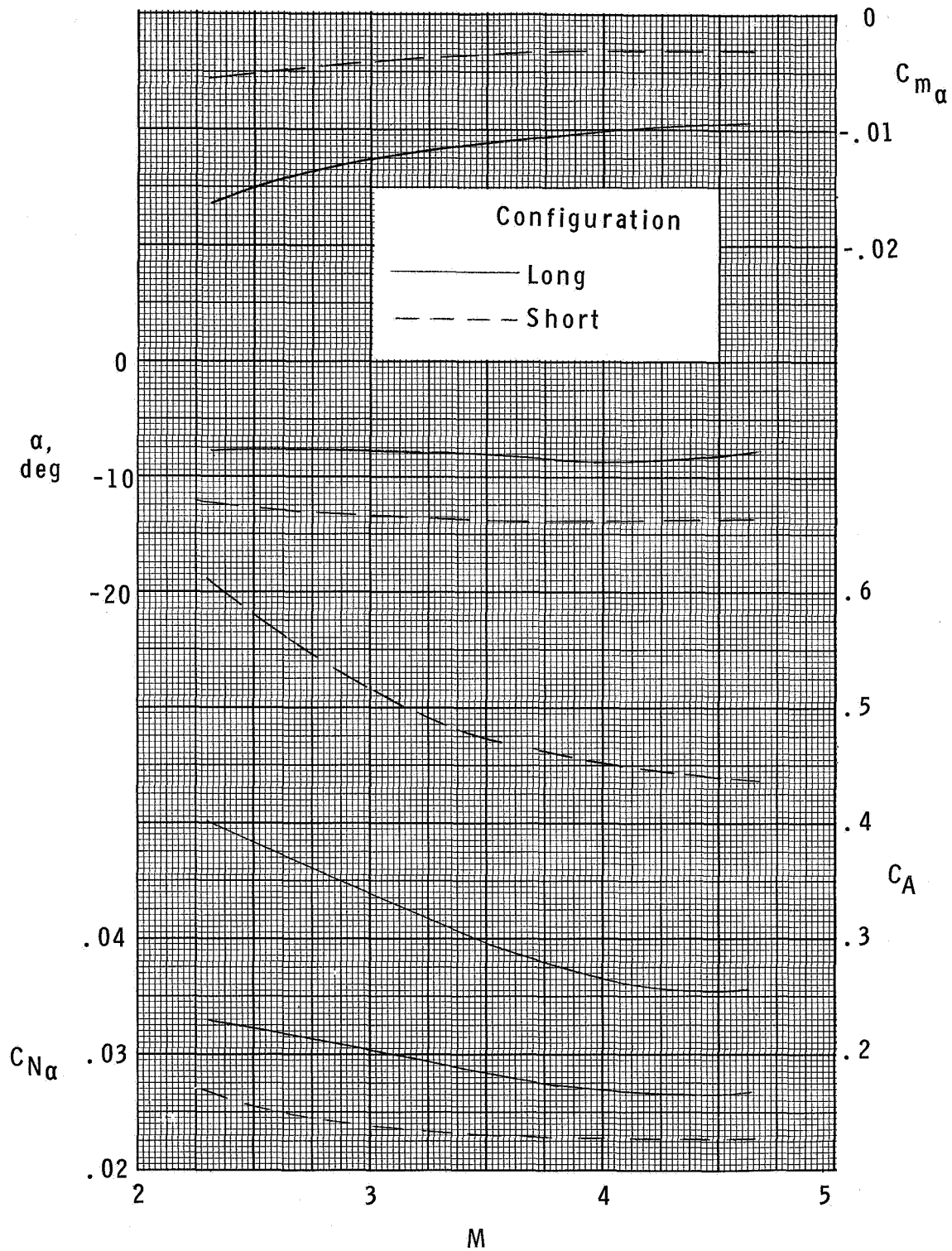


Figure 4.- Variation of longitudinal parameters with  $M$ .  $\beta = 0^\circ$ ;  $C_N = 0$ .



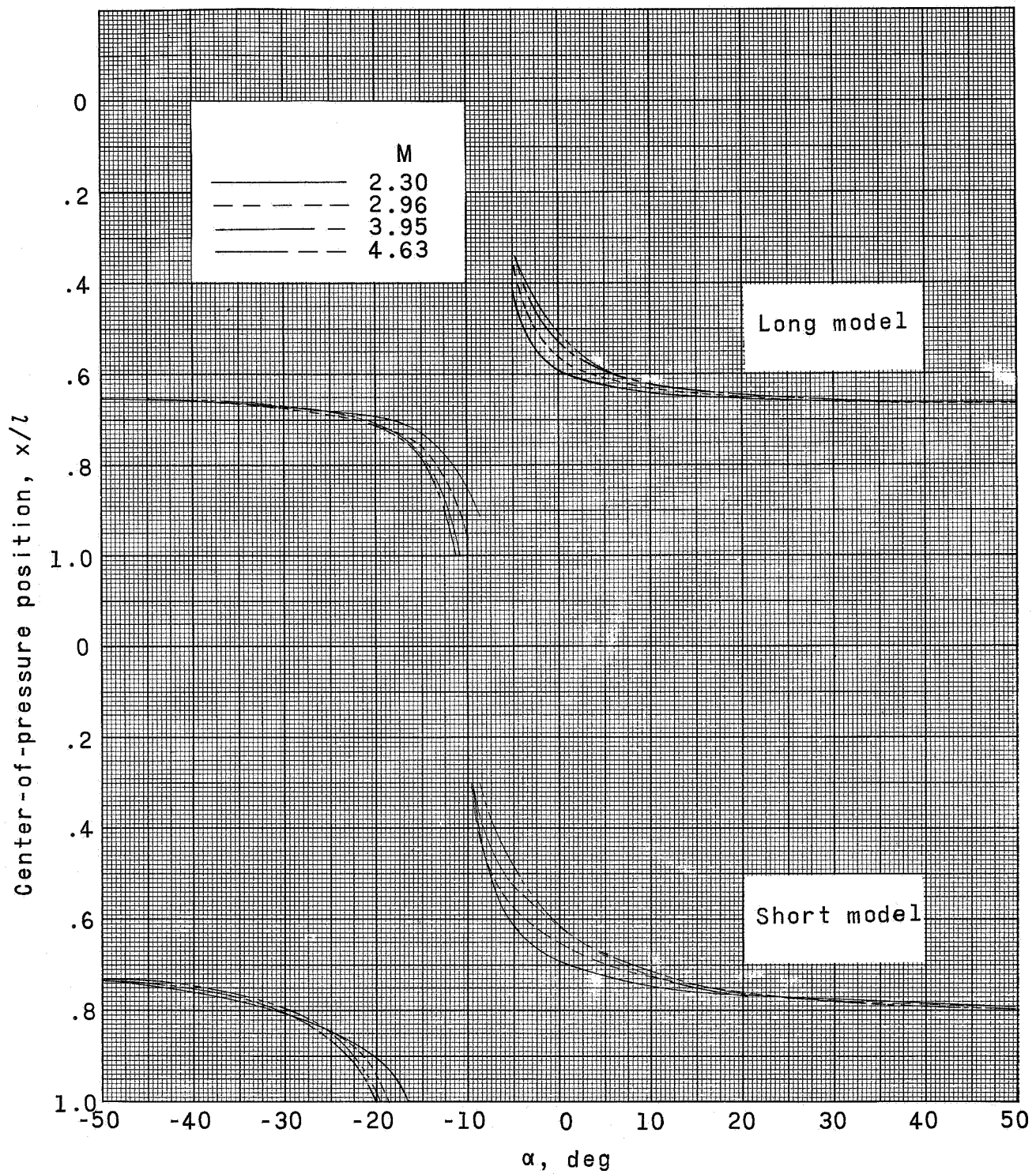


Figure 5.- Variation of center-of-pressure position with angle of attack.

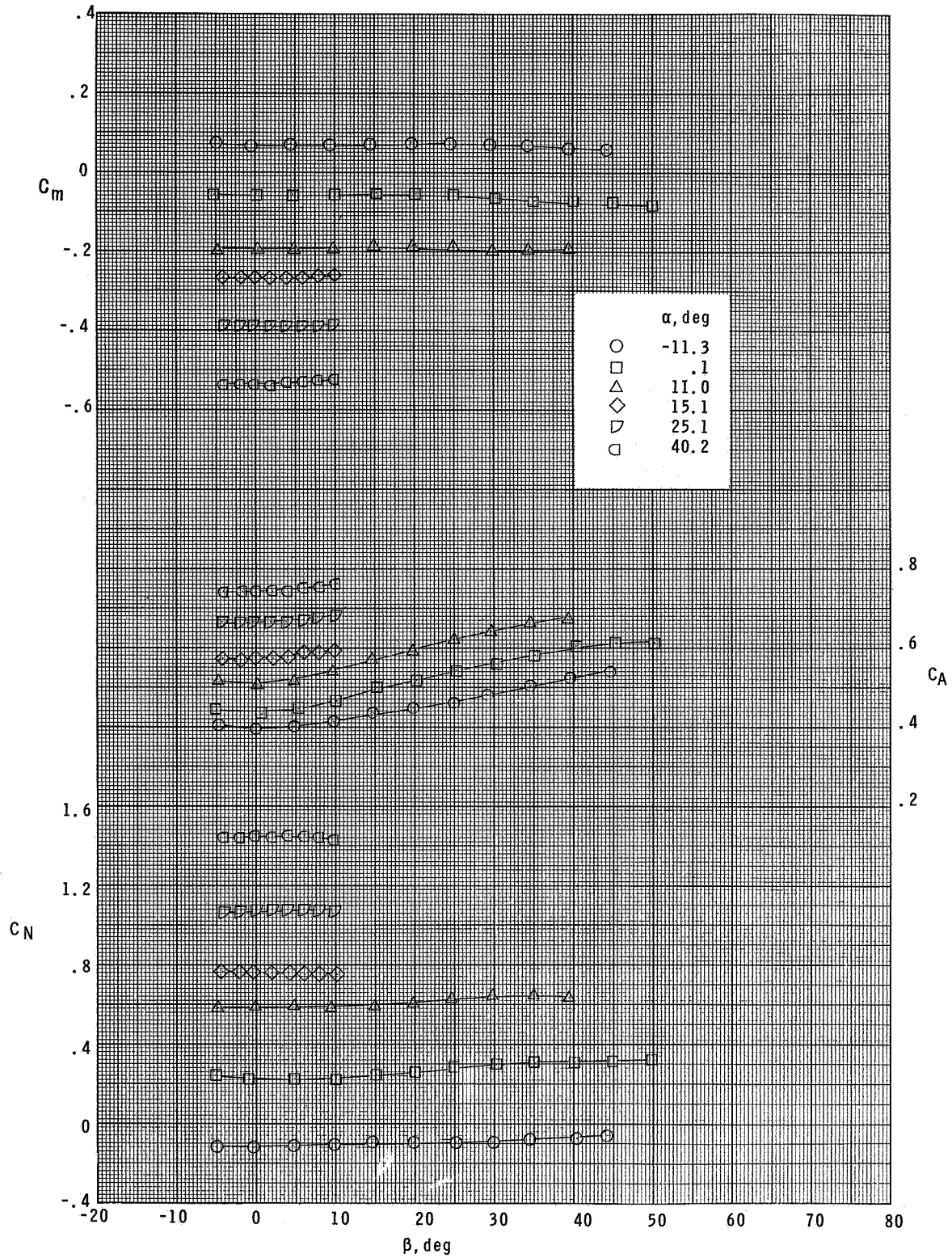


Figure 6.- Aerodynamic characteristics of long configuration in sideslip at  $M = 2.30$ .

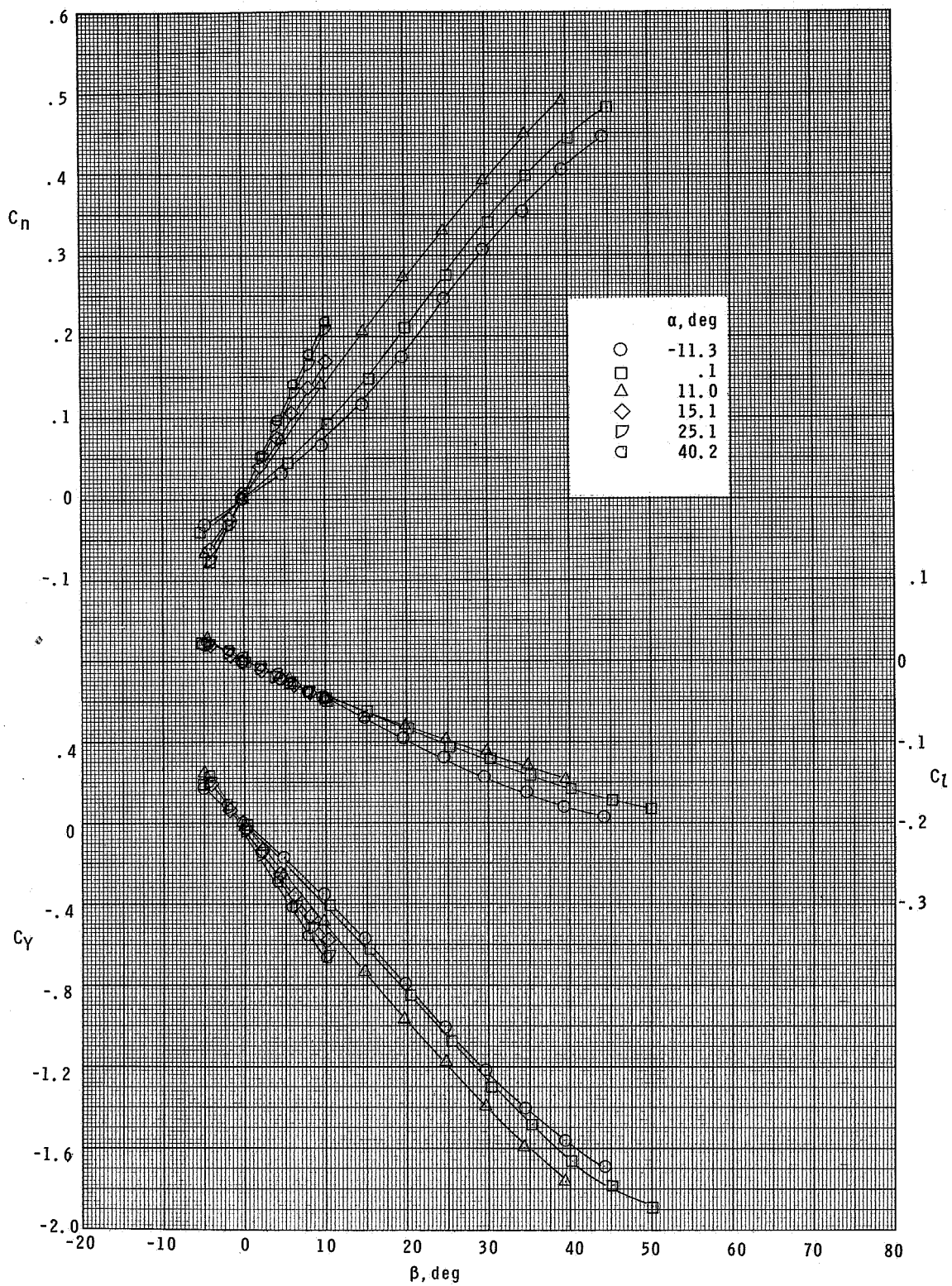


Figure 6.- Concluded.

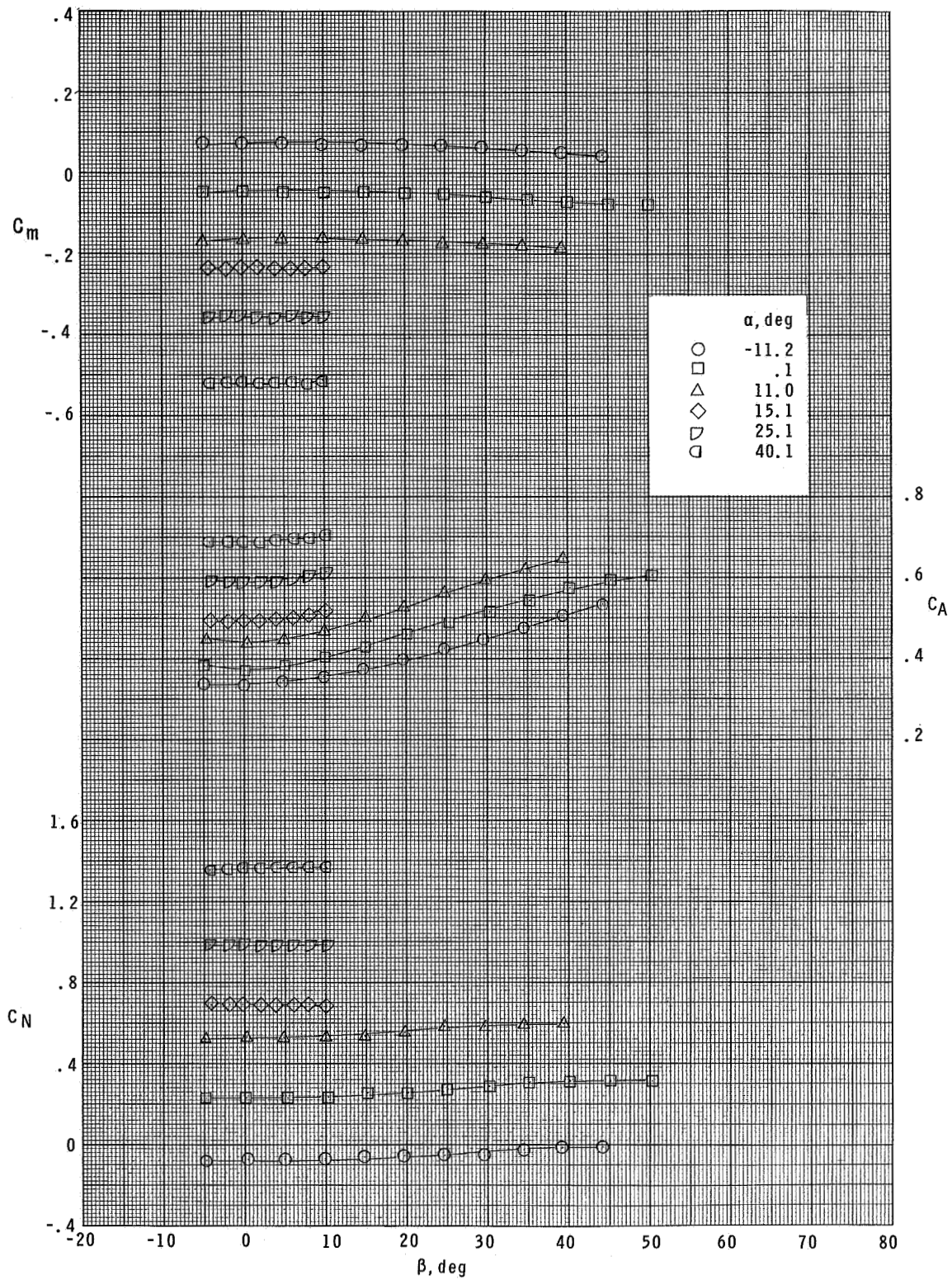


Figure 7.- Aerodynamic characteristics of long configuration in sideslip at  $M = 2.96$ .



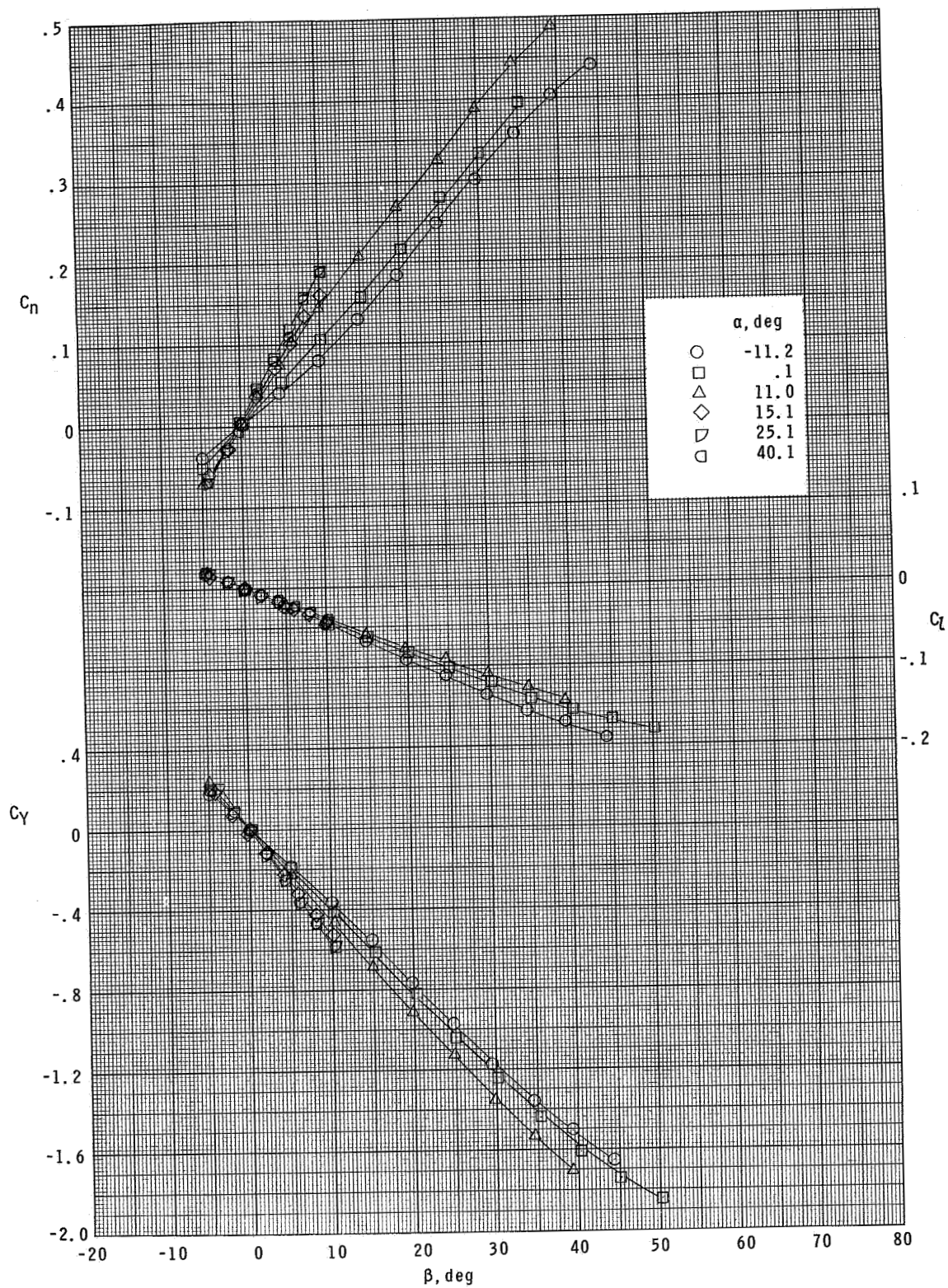


Figure 7.- Concluded.

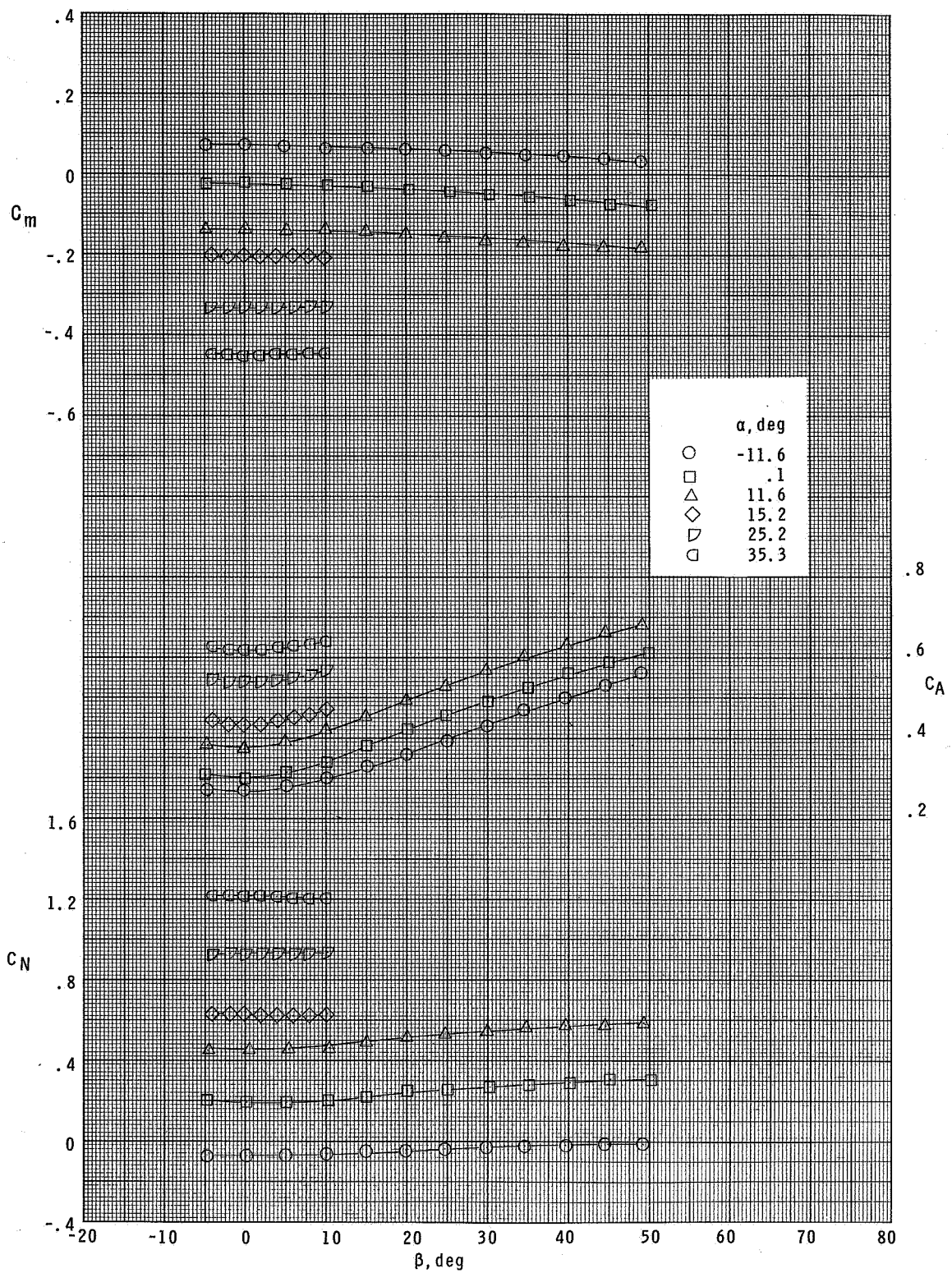


Figure 8.- Aerodynamic characteristics of long configuration in sideslip at  $M = 3.95$ .

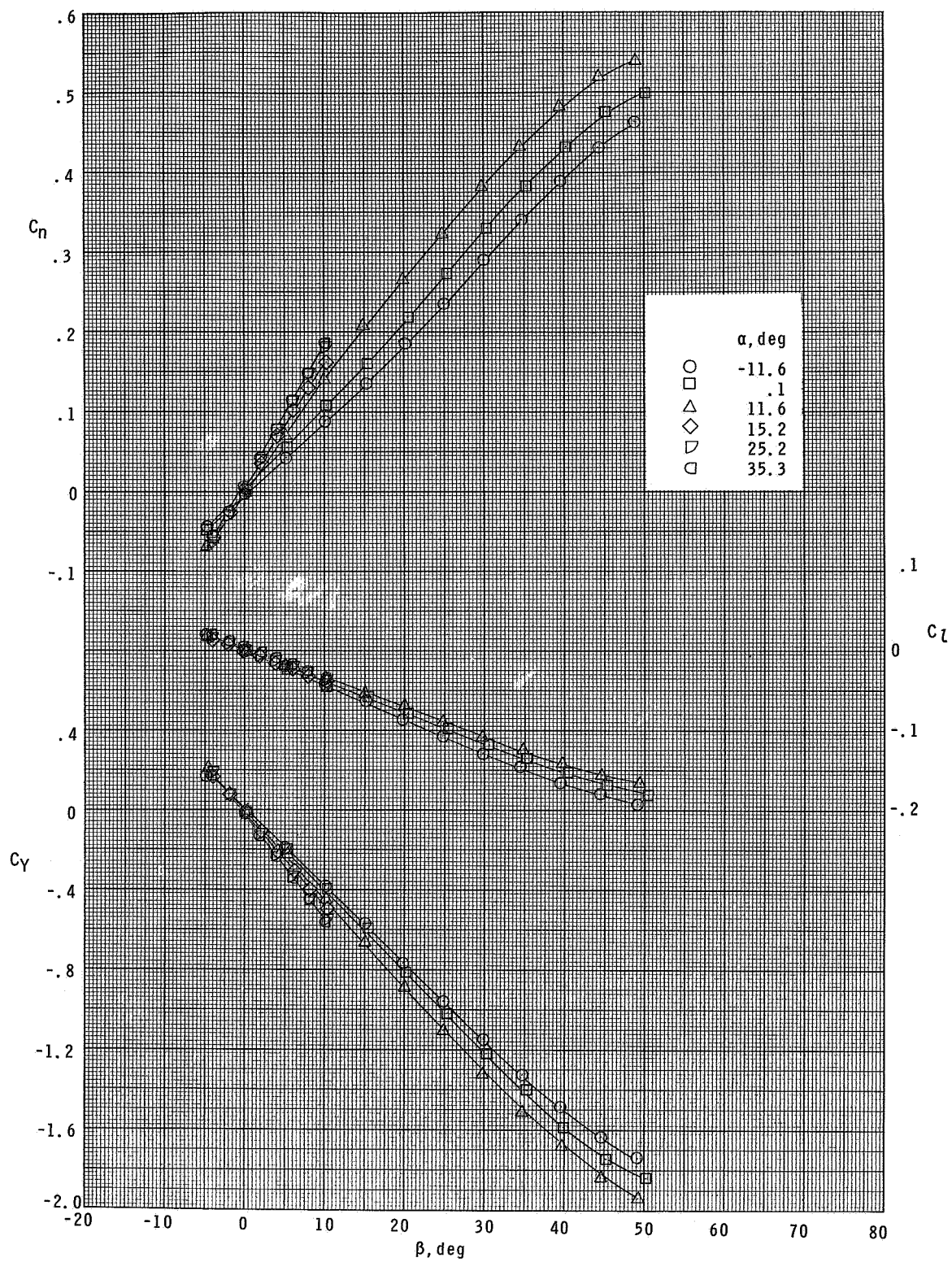


Figure 8.- Concluded.



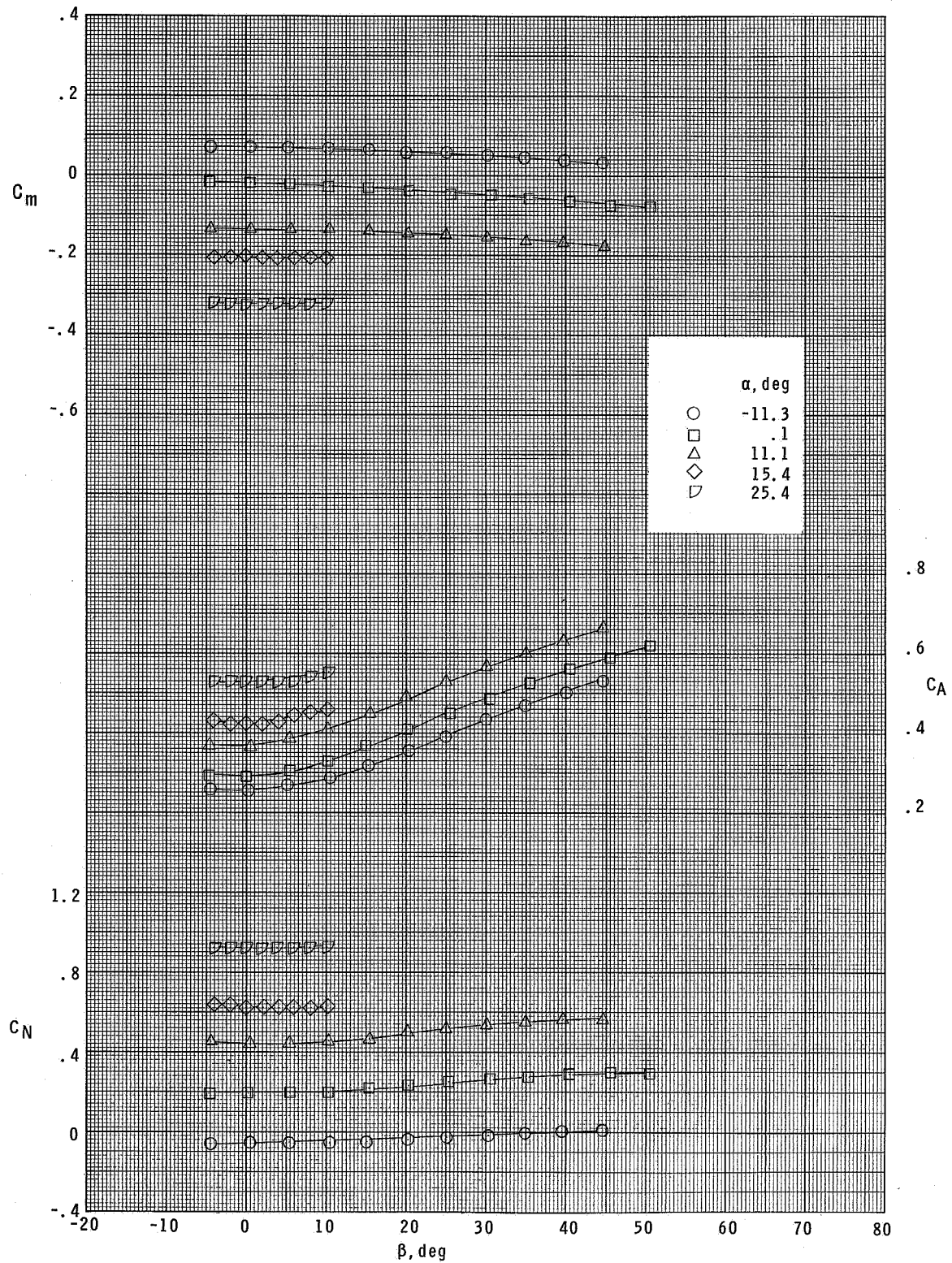


Figure 9.- Aerodynamic characteristics of the long configuration in sideslip at  $M = 4.63$ .



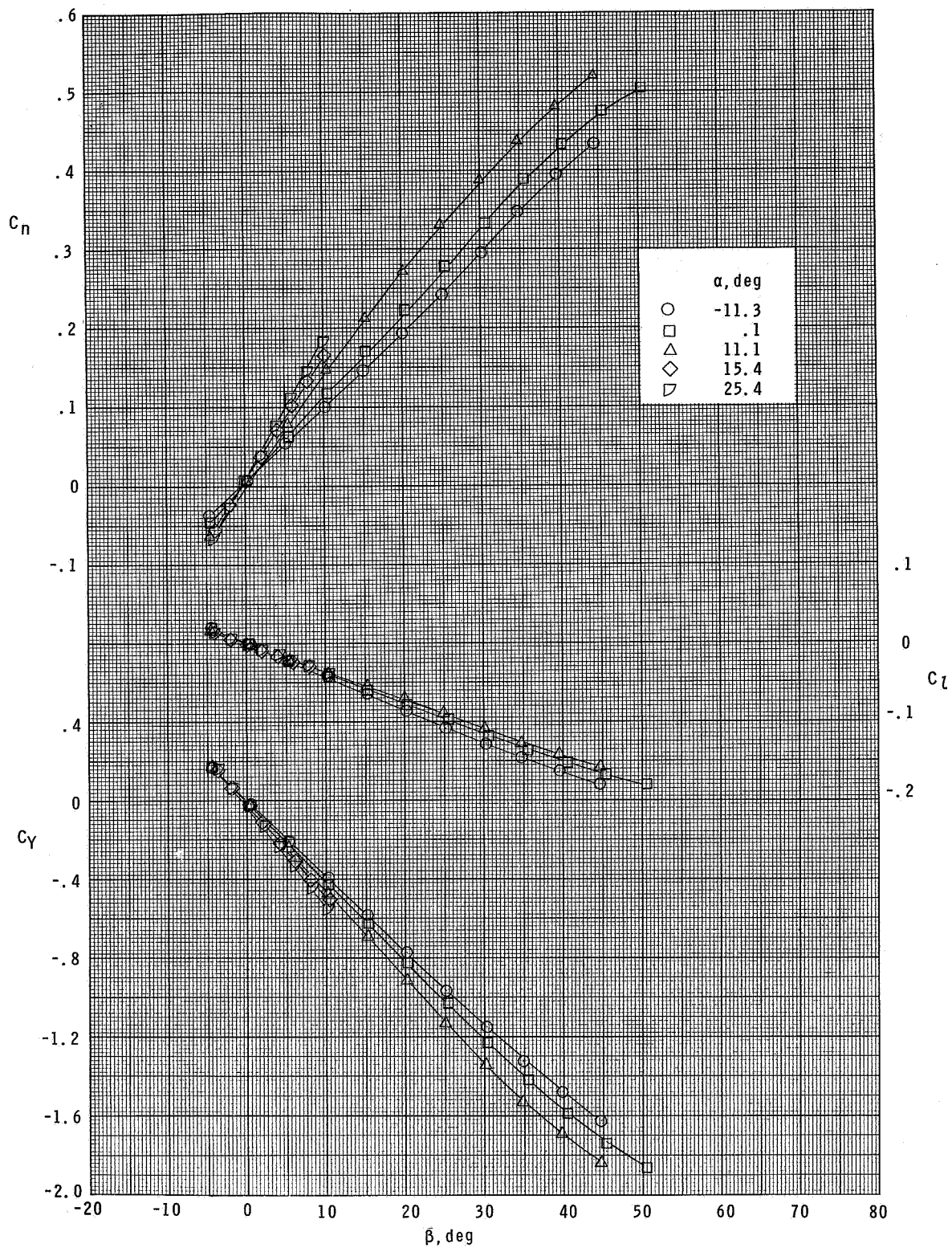


Figure 9.- Concluded.

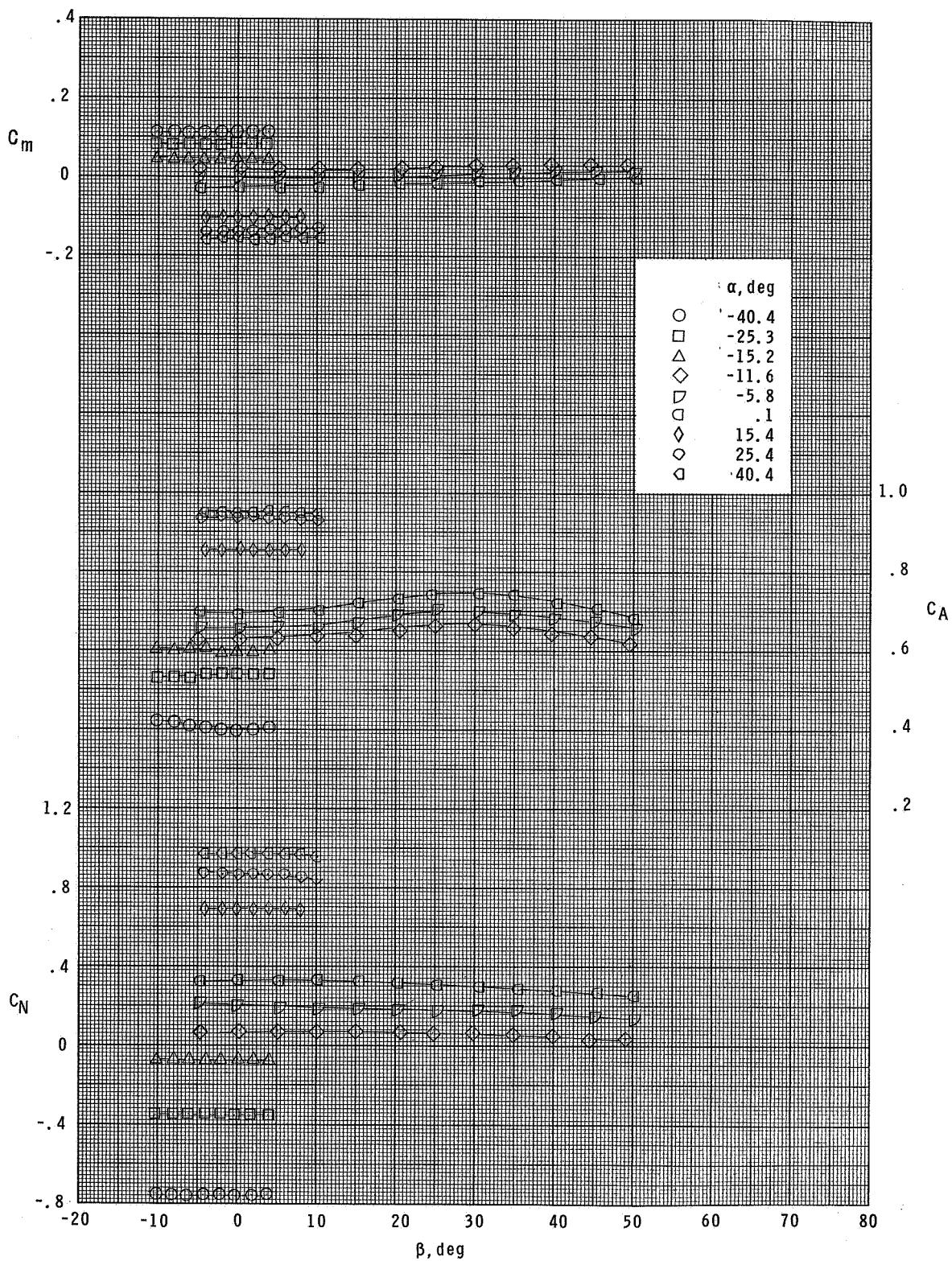


Figure 10.- Aerodynamic characteristics of the short configuration in sideslip at  $M = 2.30$ .

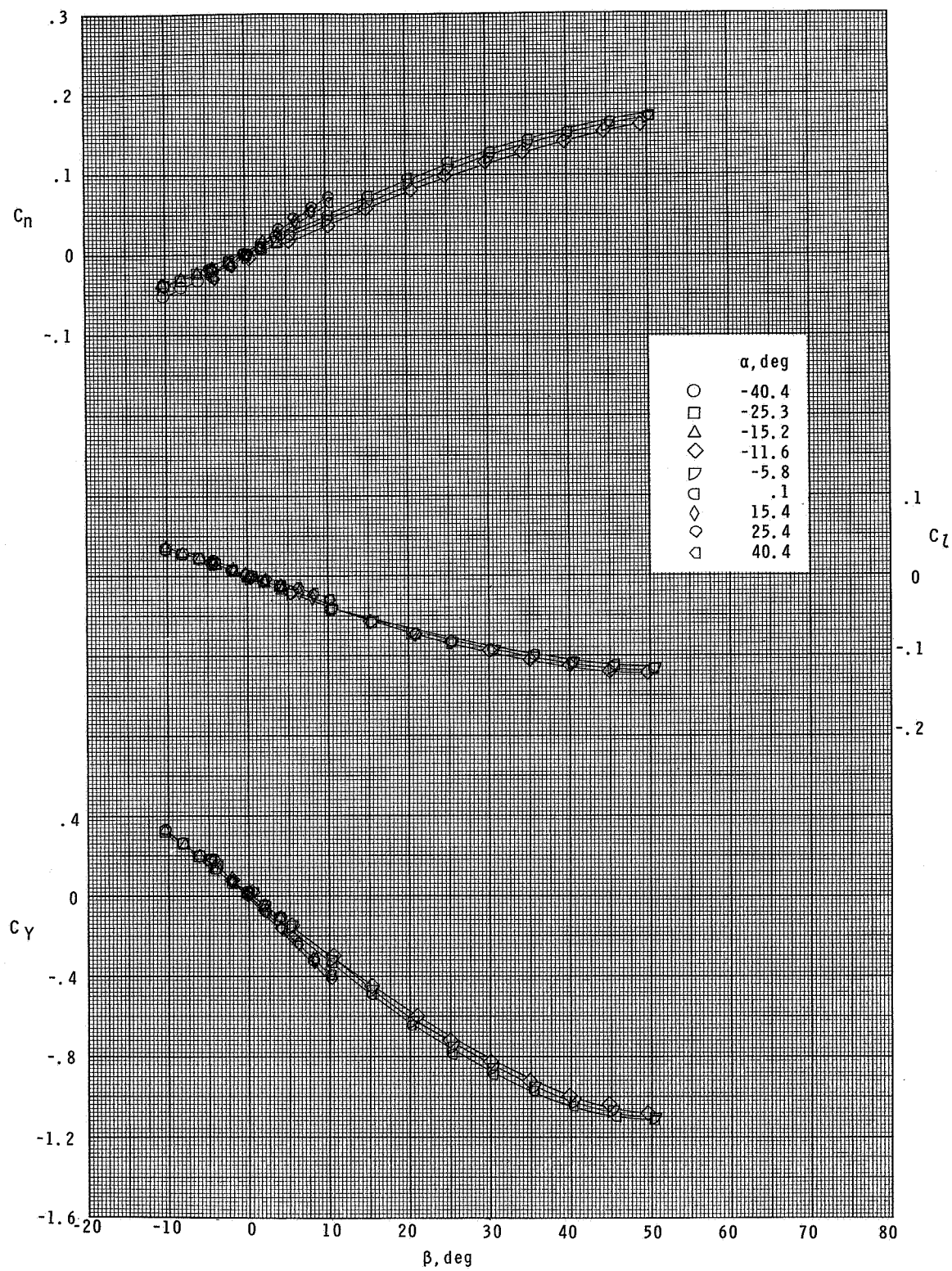


Figure 10.- Concluded.



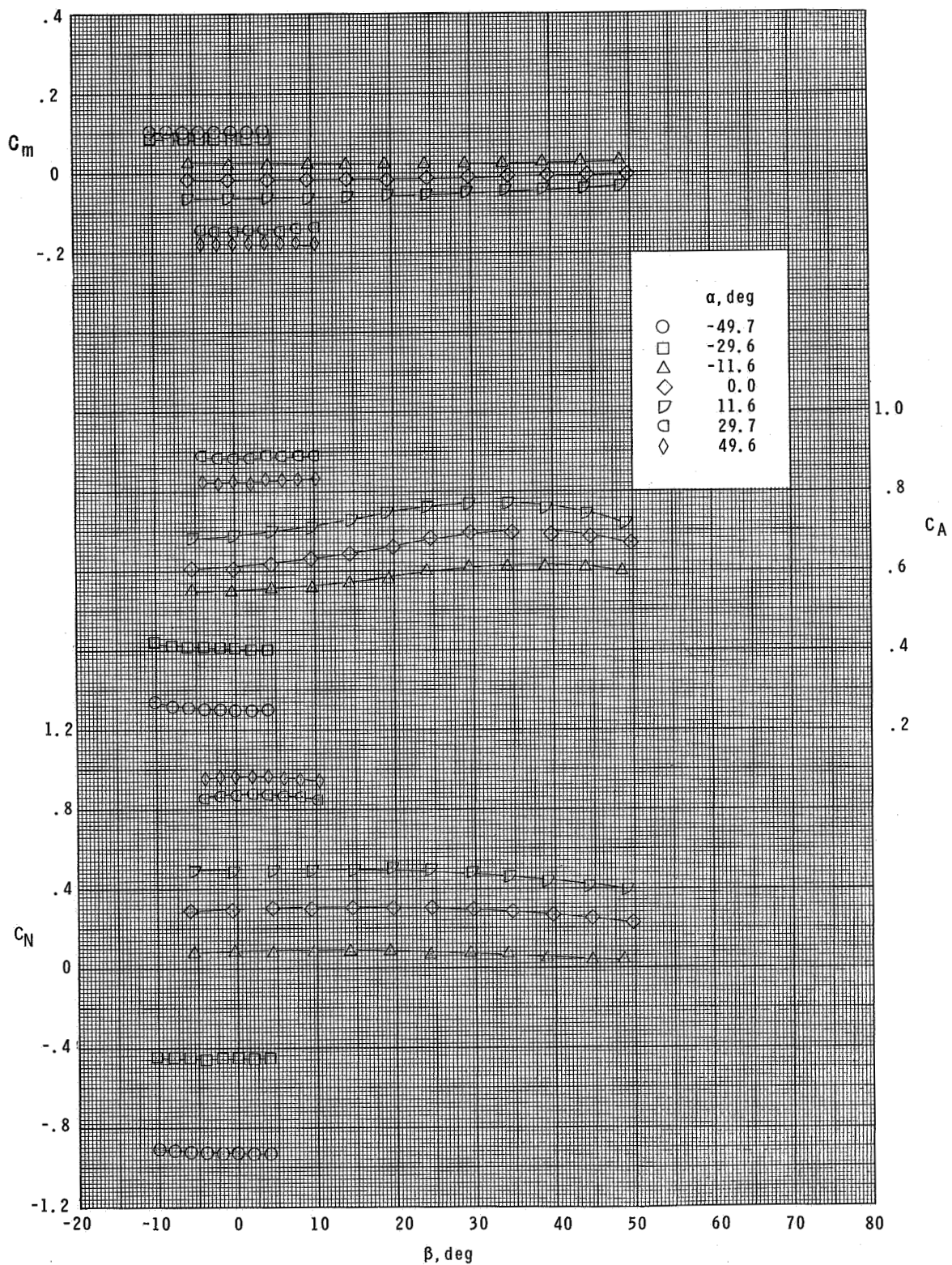


Figure 11.- Aerodynamic characteristics of short configuration in sideslip at  $M = 2.96$ .



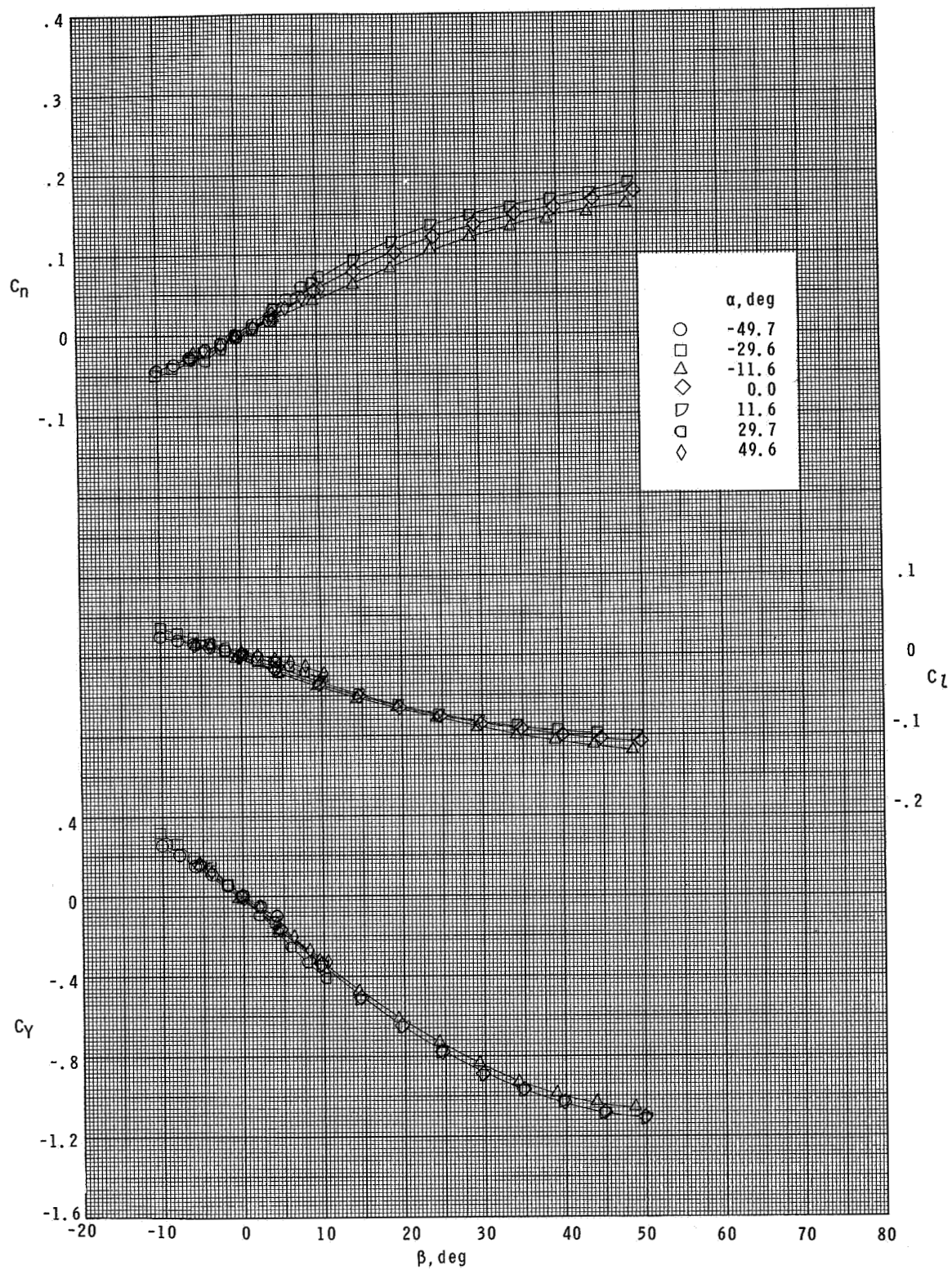


Figure 11.- Concluded.

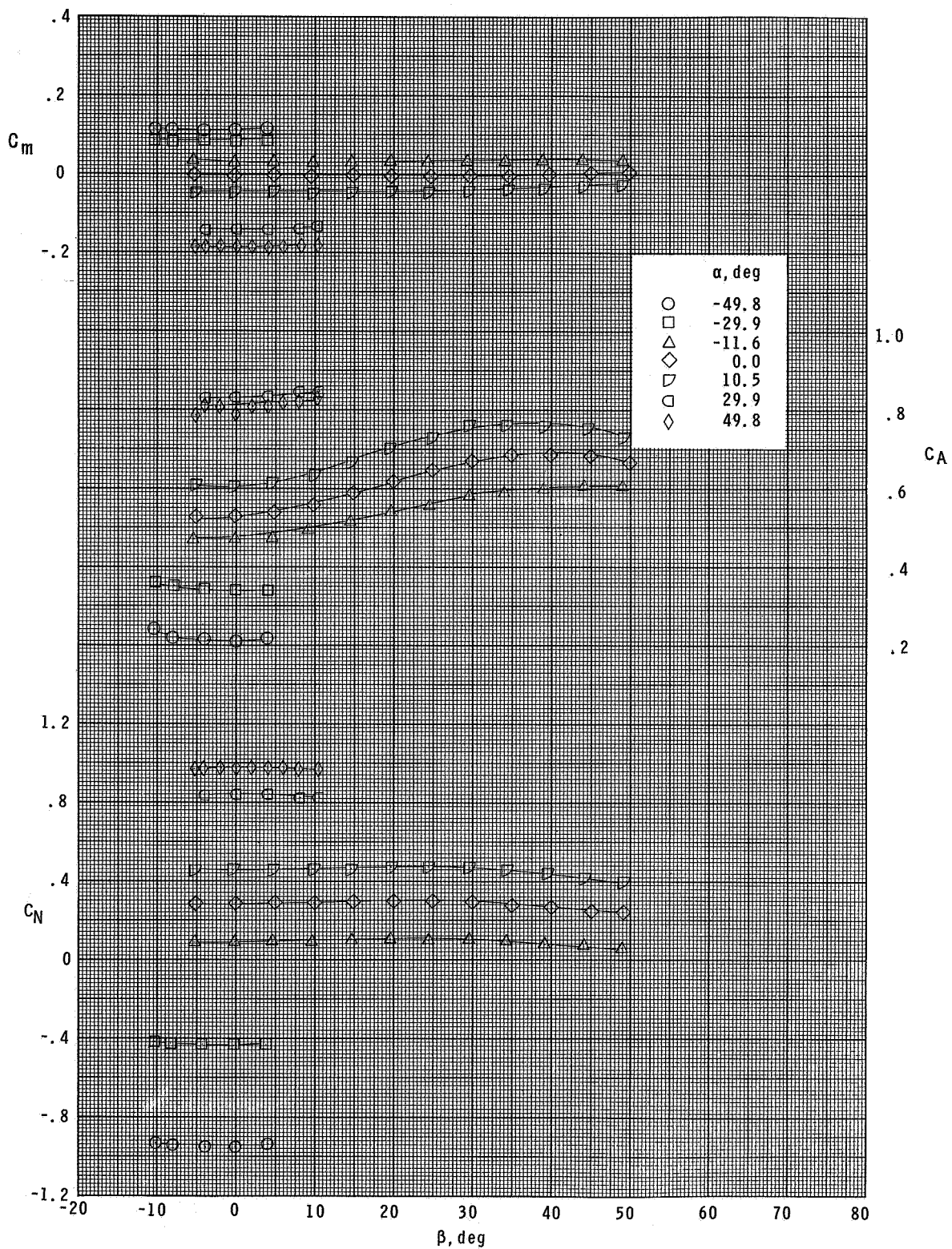


Figure 12.- Aerodynamic characteristics of short configuration in sideslip at  $M = 3.95$ .

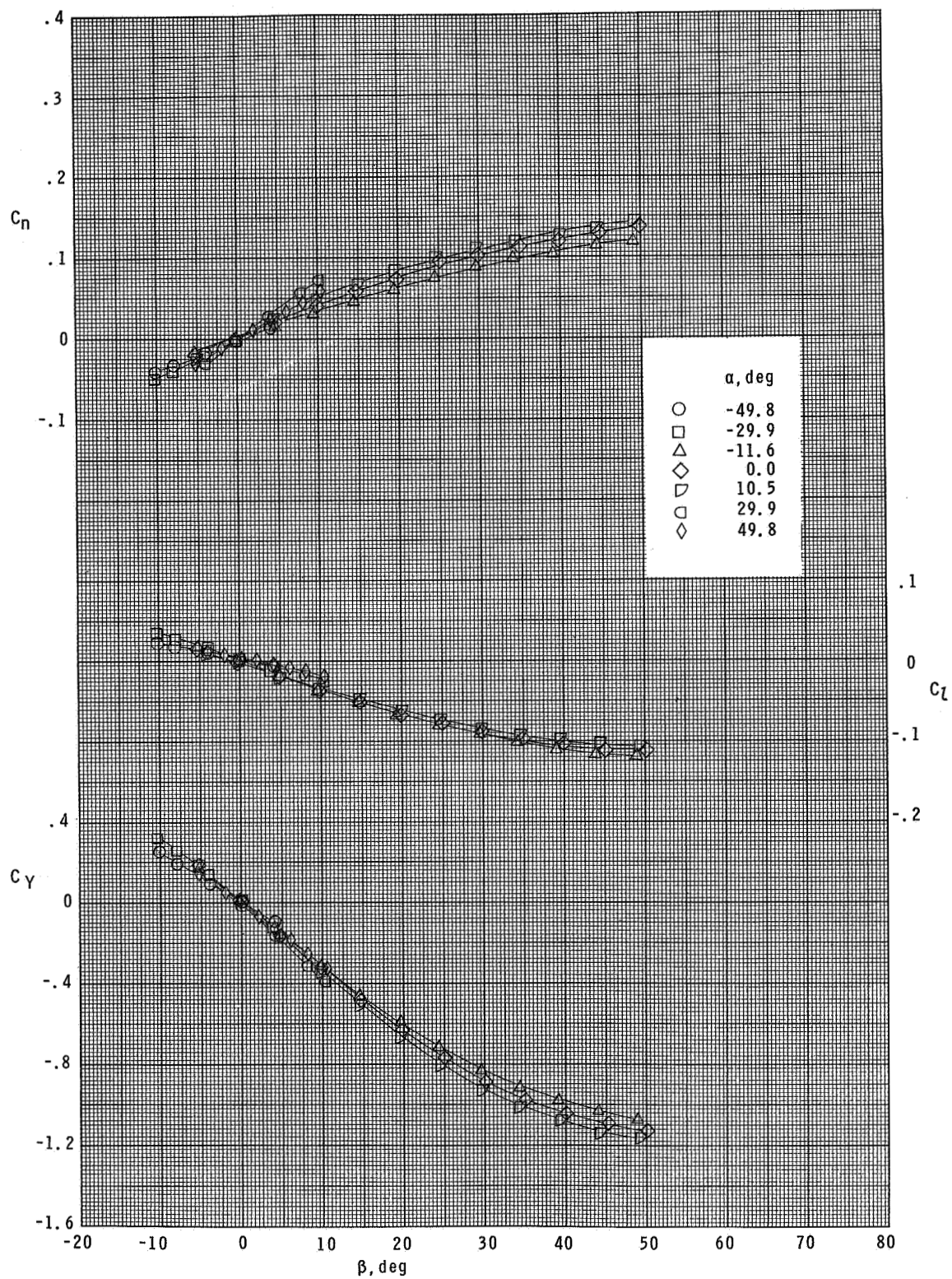


Figure 12.- Concluded.



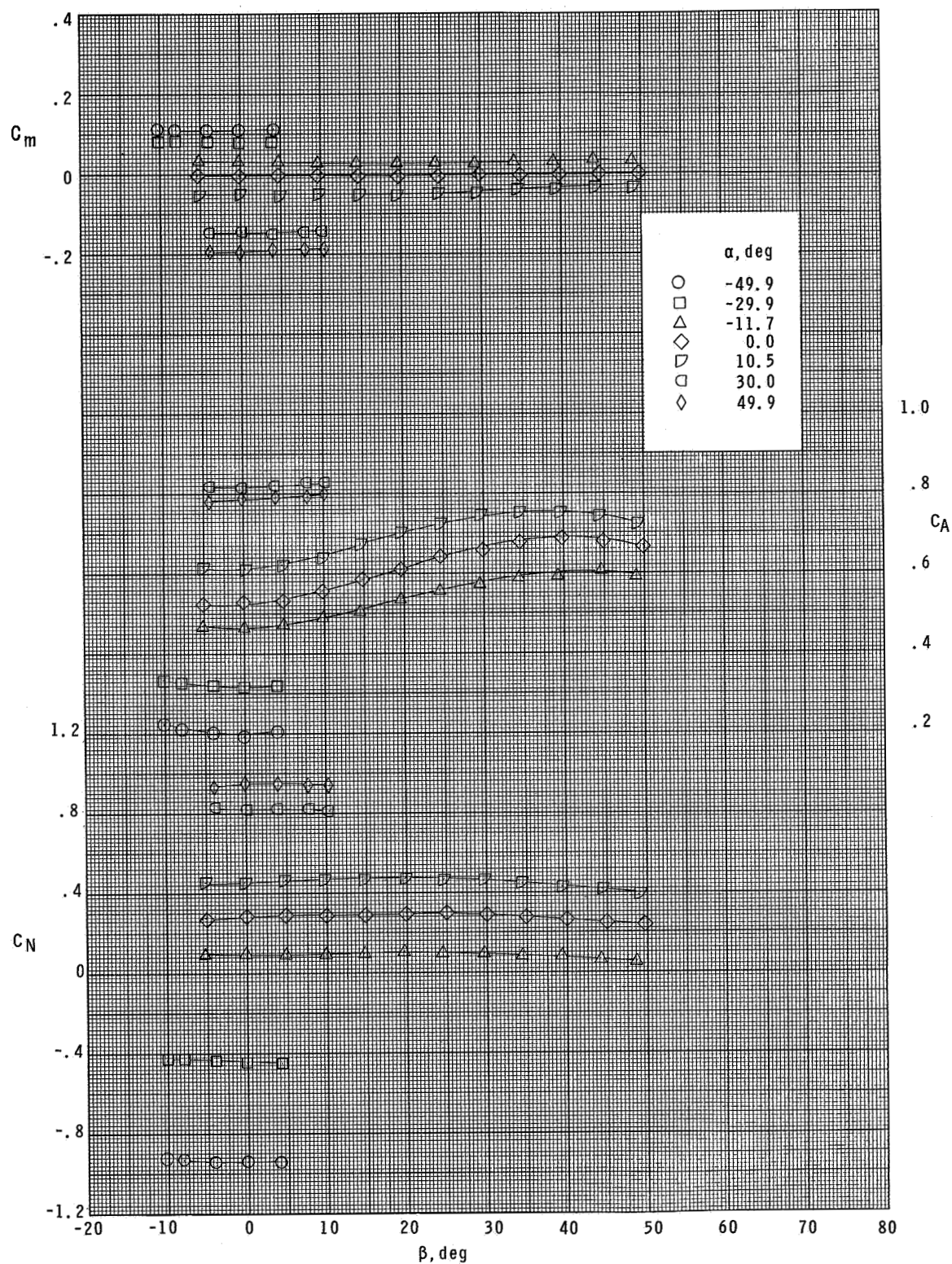


Figure 13.- Aerodynamic characteristics of short configuration in sideslip at  $M = 4.63$ .



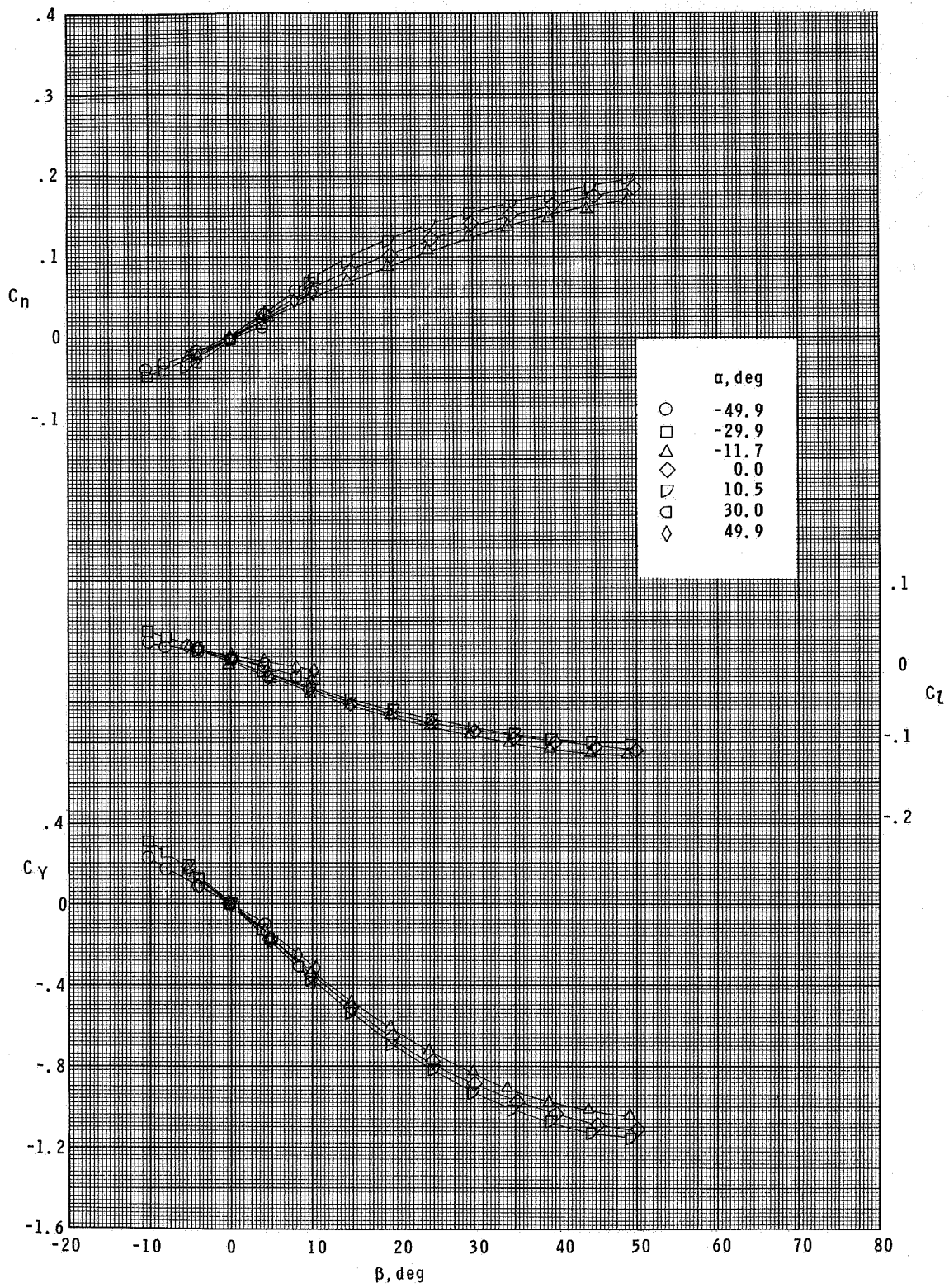
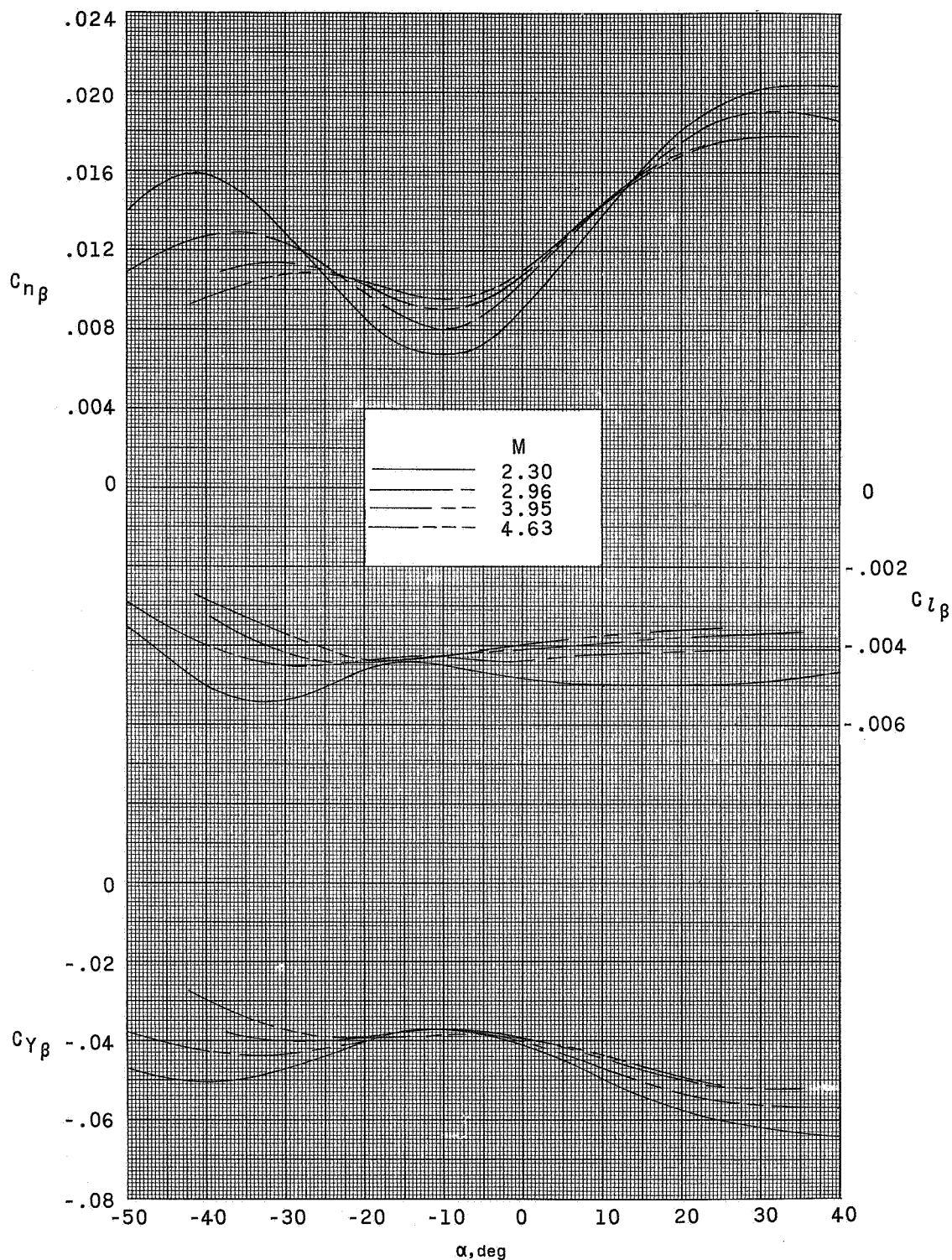
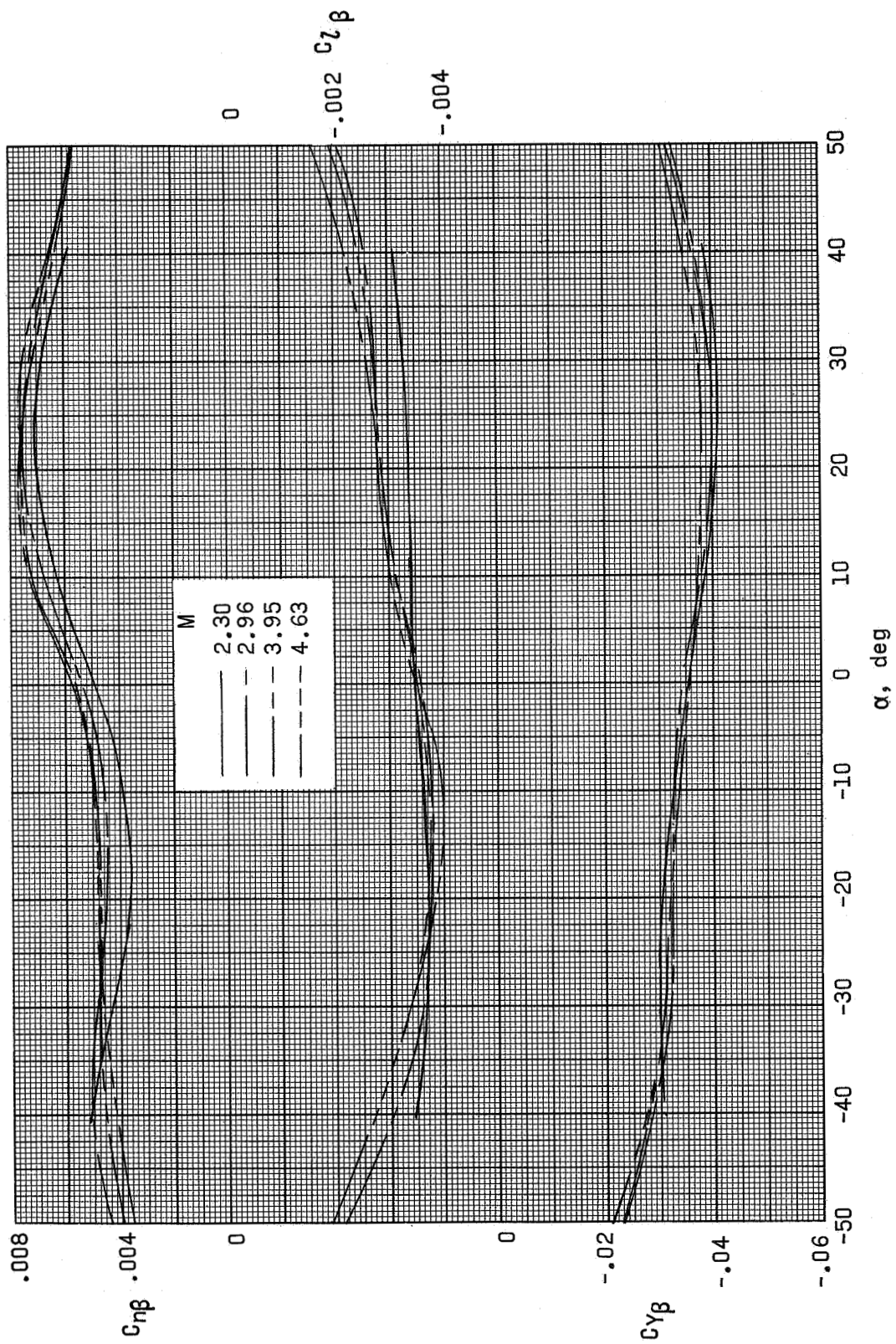


Figure 13.- Concluded.



(a) Long configuration.

Figure 14.- Variation of lateral-directional stability parameters with angle of attack.



(b) Short configuration.

Figure 14.- Concluded.